UNIVERSIDADE DE LISBOA
FACULDADE DE CIÊNCIAS
DEPARTAMENTO DE BIOLOGIA ANIMAL

A link between Primary Cilia and Gaucher disease

Bárbara Lopes dos Santos

Mestrado em Biologia Evolutiva e do Desenvolvimento

Dissertação orientada por:
Doutora Sandra Martins
Doutora Sólveig Thorsteinsdóttir

2023

Acknowledgments

Esta dissertação só foi possível através da ajuda e participação de inúmeras pessoas às quais, estarei eternamente grata por todo o apoio que me deram ao longo deste caminho por vezes repleto de inseguranças e medos.

Primeiramente, gostaria de agradecer às minhas orientadoras a Sandra, a Teresa e a Susana por me terem recebido de braços abertos neste projeto e me terem dado todo o apoio que precisei ao longo do mesmo. Gostaria de agradecer especialmente à Sandra por me ter transmitido a sua paixão pela área da investigação, pela dedicação e entusiasmo que demonstrou em cada ensinamento que me transmitiu e por todos os "puxões" de orelhas dados quando fazia alguma coisa de errado. Esteve sempre presente nos momentos bons e menos bons ao longo deste último ano, sempre pronta para me dar um abraço amigo ou para me perguntar "como estás?", sem dúvidas que estas pequenas atitudes fizeram toda a diferença, transmitiram-me segurança e confiança para dar sempre o meu melhor. Muito obrigada por terem sido umas excelentes orientadoras!

O agradecimento mais importante é dirigido aos meus pais, Célia e Paulo e ao meu irmão Afonso. Por me terem dado todo o apoio necessário, por me terem dado a possibilidade de voar e seguir os meus sonhos mesmo que por vezes não tenha sido fácil. Estiveram presentes em todos os momentos, nos bons e nos maus são os primeiros a comemorar as minhas conquistas, mas também são os primeiros a chamarem-me à razão. Muito obrigada por acreditarem e confiarem em mim e por me manterem sempre com os pés bem assentes no chão. Um especial obrigado ao meu irmão, que apesar de nem sempre se aperceber disso, foi muito importante no meu percurso foi sem dúvida uma das melhores surpresas da minha vida.

Gostaria ainda de agradecer à minha família académica especialmente à minha Madrinha, a Beatriz que esteve sempre pronta para me ajudar e ouvir mesmo que grande parte das vezes já estivesse farta de mim. Muito obrigada por todo o apoio que me deste, tanto em Évora como em Lisboa, sem ti o meu percurso académico não tinha sido o mesmo. Tal como prometido quero ainda agradecer aos meus afilhados Tatiana, João e Beatriz a quem prometi colocar o nome de cada um deles, obrigada por terem feito parte desta etapa!

Por fim, mas não menos importante, quero agradecer a todos os meus amigos mais próximos que participaram ativamente neste caminho. À Mariana, pelas inúmeras chamadas de apoio emocional, onde falamos sobre tudo, mas ao mesmo tempo sobre nada. À Sandra, Ana e Mafalda por todas as videochamadas que serviram de motivação ao estudo, por todas as brincadeiras e por me terem ouvido tantas e tantas vezes. À Madalena, que foi a minha primeira amiga da FCUL que me mostrou que afinal Lisboa até podia ser divertido, obrigada por todos os cafés e por me mostrares os melhores mexicanos da capital. Quero ainda agradecer à Laura que faz parte dos amigos que escolhemos como família, conhecemo-nos recentemente, mas ajudou-me imenso a acreditar e a confiar em mim. Muito obrigada por todo o apoio, sobretudo pela companhia no comboio!

Não sei o que virá a seguir, mas sei que estou internamente grata a todos vocês e a todos aqueles que de alguma forma ajudaram-me ao longo deste caminho, um sincero OBRIGADA!

Abstract

Gaucher disease is a lysosomal disease caused by a mutation in the *GBA1* gene. This gene encodes the lysosomal enzyme glucocerebrosidase (Gcase), which is responsible for the degradation of glucosylceramide into glucose and ceramide. Therefore, when a loss-of-function mutation occurs in the *GBA1* gene, there is an abnormal accumulation of glucosylceramide in the lysosomes, responsible for the increase in volume of lysosomes. This disease presents a very wide spectrum of phenotypic manifestations, the most frequent of which is hepatosplenomegaly, and, in some situations, there may be involvement of the nervous system. Cilia are highly conserved and complex organelles that function as chemical and mechanical sensors of cells, presenting receptors for various signaling pathways such as Sonic Hedgehog (*Shh)* on their ciliary membrane.

To try to understand which changes in genetic expression are associated with Gaucher disease, studies previously carried out in the laboratory of Prof.ª Dr.ª Maria Carmo-Fonseca compared, through RNA-seq, fibroblasts from apparently healthy individuals and individuals with Gaucher disease. Surprisingly, the bioinformatic analysis of these results showed changes in the alternative splicing pattern in a set of ciliary genes.

The objective of this project was to try to understand how lysosomal dysfunctions culminate in changes in the regulation of genetic expression of primary cilium genes and whether these are reversible after treatment of Gaucher fibroblasts with recombinant Gcase, the enzyme used in the treatment of Gaucher patients. To this end, we morphologically analyzed the ciliary membrane and axoneme of primary cilia through the Arl13b and acetylated α-tubulin staining respectively, from Gaucher fibroblasts. After morphological analysis, we verified an increase in ciliary length in Gaucher fibroblasts compared to control one, which was reversed through treatment with Gcase. We also identified anomalies in the ciliary membrane and in the cilium axoneme of Gaucher fibroblasts, related to the pattern of acetylated α-tubulin that were slightly recovered upon treatment.

Keywords: Lysosomal storage diseases, Gaucher disease, Primary cilia, Lysosome, Splicing

Resumo

As doenças lisossomais são doenças genéticas raras, autossómicas recessivas, provocadas por mutações em genes que codificam proteínas lisossomais. Estas mutações conduzem a alterações no metabolismo de degradação de moléculas no interior dos lisossomas provocando disfunções lisossomais o que, em última instância culmina com a morte da célula. A doença de Gaucher é a doença lisossomal mais prevalente, com uma prevalência estimada de 1:40,000 to 1:60,000, sendo provocada por uma mutação no gene Glucosilceramidase beta1, *GBA1*. Este gene codifica uma enzima lisossomal, a glucocerebrosidade (Gcase) que é responsável pela degradação da glucosilceramida em glicose e ceramida; assim, quando ocorre uma mutação com perda de função no gene *GBA1*, em homozigotia, há uma acumulação anormal de glucosilceramida nos lisossomas das células, responsável pelo aumento do volume dos lisossomas levando a um aumento do tamanho da célula particularmente nas células com uma intensa atividade lisossomal, como o caso dos macrófagos.

A doença de Gaucher encontra-se dividida em três subtipos clínicos: I, II e III. O subtipo I é caraterizado por uma hepatoesplenomegália (aumento do baço e do fígado), sendo este tipo o único no qual os pacientes são elegíveis para tratamento de recombinação enzimática com Gcase recombinante. Os subtipos II e III caraterizam-se por comprometimento do sistema nervoso, sendo o subtipo II uma forma aguda da doença (manifestando-se nas crianças levando à morte dos pacientes entre os 2 a 3 anos de idade), e o subtipo III uma forma crónica de Gaucher. Atualmente a terapia mais eficaz passa pela reposição enzimática com a administração da Gcase recombinante nomeadamente a Imiglucerase. Apesar da divisão clínica em subtipos, a doença é caraterizada por apresentar um espetro muito alargado de manifestações fenotípicas, não existindo uma relação bem estabelecida entre as muitas mutações existentes no gene *GBA1* e a gravidade do fenótipo apresentado. Para além disso, sabe-se que existe uma relação entre a doença de Gaucher e a doença de Parkinson, na medida em que os indivíduos que apresentam mutações, em heterozigotia, no gene *GBA1* têm uma maior predisposição para desenvolverem Parkinson numa fase tardia da sua vida. No decorrer deste projeto a Gcase utilizada foi a Imiglucerase, fornecida pelo departamento de ensaios clínicos do Hospital de Santa Maria.

Os cílios são estruturas altamente conservadas e complexas, que se projetam a partir do corpo basal da superfície celular, estando divididos em dois grupos: (1) os cílios imóveis ou sensoriais também conhecidos como cílios primários, que apresentam um rearranjo de 9+0 (9 dupletos de microtúbulos sem o dupleto de microtúbulos central) e, (2) os cílios móveis com um rearranjo de 9+2 (9 dupleto de microtúbulos que rodeiam o dupleto central). Os cílios primários apresentam sobretudo uma função sensorial química e mecânica, funcionando assim como antenas das células permitindo às mesmas receber informação do meio extracelular e convertê-lo num sinal intracelular. Estas estruturas encontram-se ancoradas à célula por via do corpo basal, de onde emergem os axonemas. À semelhança de outras estruturas celulares os cílios apresentam uma membrana constituída maioritariamente por lípidos nomeadamente por ceramida. Dentro dos cílios ainda é possível encontrar proteínas responsáveis pelo transporte de moléculas numa direção bidirecional ao longo do cílio, nomeadamente as proteínas de transporte intraflagelar (IFTs). Os cílios são constituídos por quatro partes principais, o corpo basal, a zona de transição, o axonema e a membrana ciliar. Em relação ao axonema, esta estrutura é constituída por microtúbulos compostos por α-tubulina e β-tubulina no qual o processo de acetilação da α-tubulina é responsável por manter a integridade e a estabilidade destas estruturas.

De forma a tentar perceber quais as alterações na expressão genética associadas à doença de Gaucher, o grupo da Prof.ª Dr.ª Maria Carmo-Fonseca comparou, através de RNA-seq, os fibroblastos primários de três indivíduos com Doença de Gaucher e de três indivíduos aparentemente saudáveis (controlo), tendo-se encontrado após análise bioinformática destes dados, alterações no padrão de

splicing alternativo num conjunto de genes ciliares. O *splicing* é o processo através do qual ocorre a remoção dos intrões e a ligação dos exões levando à maturação do pré-mRNA em mRNA. Durante este processo, enquanto alguns exões, os chamados exões constitutivos, são sempre incluídos no mRNA maduro, outros, os chamados exões alternativos, podem ser ou não, num fenómeno designado por *splicing* alternativo. Estima-se que este mecanismo de *splicing* alternativo, onde determinados exões presentes no pré-mRNA podem ser ou não incluídos no mRNA final, ocorra em > 90% dos transcritos humanos, levando à formação de mRNAs que irão codificar diferentes isoformas da proteína inicial, sendo este o principal mecanismo responsável pela enorme diversidade do nosso proteoma. Como se encontraram alterações no padrão de *splicing* entre fibroblastos controlo comparativamente com os de Gaucher em genes ciliares, surgiu uma parceria entre o grupo da Prof.ª Dr.ª Maria Carmo-Fonseca do Instituto de Medicina Molecular e o grupo da Prof.ª Dr.ª Susana Lopes da Nova Medical School Research, com o objetivo de esclarecer a relação entre cílios primários e doença de Gaucher.

Face ao exposto, este projeto teve como objetivo compreender de que forma disfunções lisossomais culminam em alterações na regulação da expressão genética de genes do cílio primário e se, estas são reversíveis após tratamento de fibroblastos de Gaucher com Gcase recombinante durante 5 dias. Para tal realizamos uma caraterização morfológica detalhada da membrana ciliar, através da marcação da proteína ARL13b altamente enriquecida nesta membrana, e do axonema, através da marcação por imunofluorescência da α-tubulina acetilada, dos cílios primários de fibroblastos de indivíduos portadores da doença de Gaucher. Avaliamos funcionalmente as vias de transdução de sinal associadas ao cílio primário, nomeadamente a via *Shh*, assim como os níveis de expressão das proteínas de transporte intraflagelar, em fibroblastos de indivíduos aparentemente saudáveis comparativamente com os de indivíduos portadores da doença de Gaucher. Por outro lado, validamos vários eventos diferenciais de *splicing* alternativo em seis genes ciliares (*AKNA, CDK20, IFT88, IFT122, OFD1* e *TTC23*), previamente detetados por RNA-seq.

Através da análise morfológica verificamos um aumento do comprimento ciliar nos cílios primários em fibroblastos de indivíduos portadores da doença de Gaucher comparativamente com os fibroblastos de indivíduos aparentemente saudáveis, tendo sido este fenótipo revertido após tratamento com a Gcase. Por outo lado, através da marcação por imunofluorescência com Arl13b verificamos que a membrana ciliar estava irregular em cílios primários de Gaucher. Em relação ao axonema ciliar, através da marcação por imunofluorescência da α-tubulina acetilada, observamos que em fibroblastos de pacientes de Gaucher, havia alterações no processo de acetilação da α-tubulina nomeadamente o facto da α-tubulina não estar presente ao longo de todo o cílio, existindo uma tendência para este fenótipo ser revertido através do tratamento com a Gcase. Assim, em termos morfológicos, verificamos que as alterações observadas na membrana ciliar são acompanhadas por alterações no axonema e que, após tratamento com a Gcase, apenas conseguimos reverter o comprimento ciliar, aproximando-o dos valores observados nos controlos. Associado às alterações morfológicas observadas, fibroblastos provenientes de doentes de Gaucher apresentam uma hiperativação da via de sinalização *Shh,* após ativação química desta via de sinalização.Finalmente, no decorrer deste projeto validámos ainda por qRT-PCR seis eventos do *splicing* alternativo em genes ciliares previamente identificados por RNA-Seq, demonstrando que as alterações morfológicas observadas nos cílios primários de fibroblastos de Gaucher estão acompanhadas de alterações no padrão *splicing* alternativo de genes ciliares, as últimas das quais não são capazes de serem revertidas após tratamento com Gcase.

Estudos anteriores identificaram uma relação entre o cílio primário e a doença de Niemann-Pick type C1, doença lisossomal autossómica recessiva. Nestes estudos os autores observaram alterações na morfologia do cílio relacionadas com a doença, provando assim pela primeira vez uma relação entre uma doença lisossomal e o cílio primário. Tendo isto em conta, o presente estudo é o primeiro a tentar

estabelecer uma relação entre o cílio primário e a doença de Gaucher. Apesar dos resultados obtidos não nos elucidarem acerca de qual o mecanismo molecular pelo qual alterações lisossomais culminam em alterações no cílio primário, podemos hipotetizar que as alterações observadas no cílio poderão estar relacionadas com alterações em diversos processos entre os quais o transporte intraflagelar e o processo de acetilação da α-tubulina, fruto de uma disfunção lisossomal, culminando com alterações na regulação da expressão genética de genes ciliares. No futuro, de forma a clarificar o mecanismo molecular subjacente às alterações morfológicas observadas no cílio primário mais estudos serão necessários.

Palavras-chave: Doenças lisossomais, Doença de Gaucher, Cílio primário, Lisossoma, *Splicing*

Abbreviations

AcNa - Sodium acetate

ASOs - Antisense oligonucleotides

ATAT1 - α-tubulin acetyltransferase

bp - Base Pair

cDNA - Complementary DNA

CK1 - Casein kinase 1

CO_2 - Carbon dioxide

Dhh - Desert hedgehog

DNA - Deoxyribonucleic acid

DNase – Deoxyribonuclease

dNTP - Deoxynucleotide Triphosphates

DTT – Dithiothreitol

ERT - Enzyme replacement therapy

EtOH – Ethanol

Ex – Exon

FBS - Fetal Bovine Serum

GBA1 - Glucosylceramidase beta1

Gcase – Glucocerebrosidase

GluCer – Glucosylceramide

GSK3β - Glycogen synthase kinase 3β

HDAC6 - Histone deacetylase 6

Hh – Hedgehog

HSCT - Hematopoietic stem cell transplantation

IFT - Intraflagellar transport protein

Ihh - Indian hedgehog

INPP5E - Polyphosphate 5-phosphatase

LSD - Lysosomal storage diseases

M – Molar concentration

MEM - Minimum Essential Medium

ml – Mililiters

mRNA - Messenger RNA

NPC1 - Niemann-Pick type C1

PBS - Phosphate-buffered saline

PCT - Pharmacological chaperone therapy

PFA – Paraformaldehyde

PKA - Proteins kinase A

Ptch1 - Patched1

PtdIns(4,5)P2 - Phosphatidylinositol 4,5-bisphosphate

PtdIns4P - Phosphatidylinositol-4-phosphate

PTMs - Posttranslational modifications

qRT-PCR - Real-time quantitative reverse transcription polymerase chain reaction

RNA – Ribonucleic acid

RNase – Ribonuclease

RNA-seq - RNA sequencing

rpm - Rotations per minute

RT – Room temperature

SAG – Smoothened agonist

Shh – Sonic Hedgehog signaling pathway

SIRT2 - Sirtuin type 2 deacetylase

Smo – Smoothened

snRNA - Small nuclear RNA

SNT - Simple neurite tracer

SRT - Substrate reducing therapy

SUFU - Suppressor of Fused

U – Units

WT – Wild type

µl – Microliters

µm – Micrometers

Contents

Chapter 3. Results

List of Tables

List of Figures

Chapter 1. Introduction

1.1. Lysosomal storage diseases (LSD)

Lysosomal storage diseases (LSD) are a group of 70 rare, autosomal recessive genetic diseases caused by mutations in the genes that encode lysosomal proteins[1]. These diseases have an estimated prevalence of 1:5000 to 1:5500 and may be more prevalent in some populations, such as Ashkenazi Jews[1]. LSD-causing mutations lead to alterations in the metabolism of degradation of molecules in lysosomes, which causes lysosomal dysfunction, leading to an accumulation of substrates within the lysosomes, causing cell dysfunction and death, which ultimately may lead to dysfunction and degeneration of the organ affected[1]. Lysosomes are cellular structures responsible for the degradation and recycling of macromolecules such as carbohydrates, proteins, nucleic acids, and lipids once these molecules reach lysosomes through endocytosis, phagocytosis, or autophagy[2]. Thus, lysosomes play a fundamental role in maintaining cellular homeostasis through the process of autophagy[1,3].

Clinically, LSD are quite heterogeneous and can affect different organs and systems, such as the liver, spleen, cardiovascular system, central nervous system, which is very sensitive to lysosomal dysfunction, among others[1,4]. The diagnosis is made based on the symptoms experienced by the patient and confirmed through analysis of enzymatic activity and genetic sequence[1,5]. Regarding treatment, there are several therapies available such as substrate reducing therapy (SRT), which reduces the synthesis of accumulated substrates, hematopoietic stem cell transplantation (HSCT), where the patient is transplanted with healthy cells that will secrete the missing enzyme, the pharmacological chaperone therapy (PCT) that corrects the metabolic process through improves the activity of the dysfunctional enzyme and enzyme replacement therapy (ERT), which is currently the most used[1,5–7]. Considering that most LSDs lead to impairment of the central nervous system, currently one of the biggest challenges in relation to the treatment of these diseases is the fact that the treatments do not pass through the blood brain barrier, making them ineffective for many LSDs[4].

1.1.1. Gaucher disease

Gaucher disease is a rare, autosomal recessive lysosomal disease caused by a mutation in the glucosylceramidase beta1 (*GBA1*) gene[8]. This disease is considered the most prevalent lysosomal disease, with an estimated prevalence of 1:40,000 to 1:60,000, with a high incidence (approximately 1:800) in the Ashkenazi Jewish population[8]. The *GBA1* gene, located on chromosome 1q21, encodes the lysosomal enzyme glucocerebrosidase (Gcase), responsible for the degradation of glucosylceramide (GluCer) into glucose and ceramide[8]. Thus, loss-of-function mutations in the *GBA1* gene, in homozygosity, lead to an abnormal accumulation of glucosylceramide inside the lysosomes, leading to these cells being called Gaucher cells[9,10]. This accumulation causes lysosomes to increase in size, leading to a displacement of the nucleus and, consequently, to a morphological change in the cytoplasm[9,10]. These changes are particularly evident in cells where lysosomal activity is intense, such as macrophages and other cells with high phagocytic activity.[9,10]

There are three clinical subtypes of Gaucher disease: I, II and III[8,10]. Subtype I, the most common, corresponding to ~ 90% - 95% of Gaucher patients, is characterized by hepatosplenomegaly (enlargement of the spleen and liver)[8,10]. Subtypes II and III are characterized by impairment of the nervous system, with subtype II being an acute form of the disease (manifesting itself in children,

causing patients to have an estimated average life expectancy of 11.7 months), and subtype III a chronic form of the disease[10]. However, despite the clinical division into subtypes, the disease is characterized by a very broad spectrum of phenotypic manifestations, and there is no well-established relationship between the many mutations found in the *GBA1* gene and the severity of the phenotype presented[8].

1.1.1.1. Diagnosis

Diagnosis involves a multidisciplinary approach that begins with a clinical evaluation, in which the patient must present at least two of the following symptoms: hepatosplenomegaly, anaemia, thrombocytopenia, bone lesions and central nervous system involvement[11,12]. Additionally, the activity of the lysosomal enzyme glucocerebrosidase is analysed in peripheral blood leukocytes, being the disease diagnosis confirmed each time enzymatic activity proves to be less than 15% of normal activity (normal enzymatic activity values differ between laboratories)[11,12]. To complement the diagnosis, several biomarkers are also tested, with glucosylsphingosine being considered the most sensitive and specific both for diagnosis and for analysing the response to treatment[11,12]. Other tests may also be carried out, such as ultrasonography, radiography, dual-energy x-ray absorptiometry, echocardiography, electroencephalogram, abdominal magnetic resonance imaging cap marrow aspiration, liver biopsy, and even a molecular analysis that involves sequencing the *GBA1* gene to detect mutations associated with Gaucher[11,12]. Regarding prenatal diagnosis, two types of samples can be used, chorionic villus or amniotic fluid cells, which are then subjected to genetic analysis[11,12].

1.1.1.2. Treatment

The most effective approach in the treatment of Gaucher is ERT with recombinant Gcase, namely, Imiglucerase produced through mammary cells from the Chinese hamster ovary, by the Genzyme laboratory, commercially known as Cerezyme[13].

Commercially, Imiglucerase is available in its lyophilized state, where, after dilution, each vial contains 400 units (U) of Imiglucerase per 10 millilitres of solution[14]. Only patients diagnosed with Gaucher type I and type III, if they present non-neurological manifestations such as anaemia, thrombocytopenia, or hepatosplenomegaly, are eligible for treatment with Imiglucerase[14]. Regarding its administration, this is done intravenously, with a frequency of every 2 weeks and a dose of 60U/Kg; however, these values can be adapted to each patient after a medical evaluation[14].

Through clinical tests, it was possible to verify that after 1 to 2 years of treatment with Imiglucerase, there was an improvement in the symptoms experienced, including a decrease of 30%-50% and 20%-30% in the volume of the spleen and liver, respectively, together with an increase in haemoglobin and platelet levels[13].

1.1.1.3. Relationship between Gaucher disease and Parkinson’s disease

Due to the strong lysosomal presence in neurons, namely in neuronal cell bodies, dendrites, and axons, the lysosomal system plays an important role in the neurodegenerative process, making the central nervous system of LSD patients more sensitive to lysosomal dysfunction[15,16]. Thus, although it is not yet well established, it is known that there is a relationship between Gaucher and Parkinson's diseases, as individuals who present heterozygous mutations in the *GBA1* gene and patients who present the Gaucher subtype I, have a greater predisposition to develop Parkinson's later in life[12,17].

Parkinson's disease is a neurodegenerative disease characterized by the degeneration of dopaminergic neurons and the presence of Lewy bodies in neurons, presenting mainly motor symptoms, such as muscle stiffness and movement difficulties, despite non-motor symptoms, such as dementia, may also be present[17,18]. Lewy bodies are abnormal clusters of proteins whose main component is the protein α-synuclein[19]. It is currently believed that the relationship between Parkinson's and the *GBA1* gene is directly related to the protein α-synuclein, and there is evidence that indicates that the decrease in glucocerebrosidase activity leads to a pathological worsening of Lewy bodies, thus increasing the risk of the patient developing Parkinson's[19].

In recent years, the α-tubulin acetylation process has been implicated as having an important role in several neurodegenerative diseases such as Parkinson's, and it has been demonstrated that Parkinson's patients present a decrease in the α-tubulin acetylation process[20]. Microtubules, present in neuronal cells, play a crucial role in the transmission of information, in the formation of the ciliary axoneme and in the maintenance of the cytoskeleton of neuronal cells, causing dysregulations in microtubules to be associated with neurodegenerative diseases[20]. On the other hand, the α-tubulin acetylation process contributes to increasing the resistance of microtubules, giving them flexibility, resistance to tension and the ability to recover from damage[20]. Considering this, it is possible to suggest that alterations in the α-tubulin acetylation process may lead to neurodegenerative processes contributing to the development of neurodegenerative diseases such as Parkinson's [20].

1.2. Primary cilia

Primary cilia are highly conserved and complex structures that project from the basal body of the cell surface[21]. These structures are formed during the G1/G0 phases, through a process called ciliogenesis, which is regulated by sphingolipids, especially ceramide[22–24]. In cell culture, the formation of cilia may be induced by placing the cells in starvation serum, as this process allows cells to return to the G1/G0 phases, leading to the formation of the cilium[22–25]. Recently, fit was found that the autophagy process, also induced by starvation serum, contributes to ciliogenesis through the degradation of several proteins, such as *OFD1*[25].

The ciliary axoneme has 9 doublets of microtubules that surround the central area of the primary cilium (in the case of motile cilia, these have an additional central pair of microtubules)[26]. Each doublet of microtubules has two tubules, the incomplete one (made up of β-tubulin) and the complete one (made up of α-tubulin) from which external and internal dynein arms are projected that function as cilia motors as they have ATPases in its constitution; in addition, the internal arms of microtubules are essential for controlling rhythmic ciliary beating, being part of the nexin-dynein regulatory complex[21,27]. Notice that cilia are divided into two groups: (1) motile cilia, with a 9+2 microtubule rearrangement, which play an important role in cell movement; notice that within this group we find a subgroup classified as nodal cilia with a 9+0 rearrangement involved in moving fluids, such as the nodal flow or the mucus clearance in our respiratory system and (2) primary cilia, also known as immotile or sensory cilia, which present a rearrangement of 9+0 microtubules, having a chemical and mechanical sensory role, functioning as “antennas” of the cells, allowing them to receive information from the extracellular environment and convert it into an intracellular signal (Fig.1.1)[26].

Thus, the primary cilium plays a role in several cellular processes, namely differentiation, proliferation, migration, cell cycle control, and autophagy, but also with some signalling pathways such as the Sonic Hedgehog (*Shh*) pathway[28,29]. Mutations in genes that encode essential proteins in the

structure and functioning of the cilium cause ciliary dysfunctions that lead to ciliary diseases called ciliopathies[29,30].

1.2.1. Structure

Structurally, the cilium is made up of four main parts (Fig.1.1): (1) the basal body composed of 9 triplets of gamma tubulin responsible for anchoring the cilium to the cell surface, (2) the transition zone, where the microtubules are no longer organized in triplets, as in the basal body, and become organized in doublets, being the area responsible for controlling the entry and exit flow of ciliary molecules (3) the axoneme that function as the cytoskeleton of the cilium and (4) the ciliary membrane that covers the entire axoneme; this specialized membrane is mainly made up of sphingolipids, particularly glycosphingolipids and ceramide, having a different phospholipid constitution than the plasma membrane as the predominant phospholipid in the ciliary membrane is phosphatidylinositol-4-phosphate (PtdIns4P) while in the plasma membrane it is phosphatidylinositol 4,5-bisphosphate (PtdIns(4,5)P2), also present in the ciliary base[22,23,29–32]. The presence of the PtdIns4P phospholipid in the ciliary membrane is maintained thanks to polyphosphate 5-phosphatase (INPP5E); if INPP5E is not present, the PtdIns4P phospholipid is replaced by PtdIns(4,5)P2, which causes a deregulation of Hedgehog signaling[32]. Furthermore, the ciliary membrane also has several specific transmembrane receptors for various signalling pathways, namely the Sonic Hedgehog (*Shh*) one[22,23,29–32]. Thus, when the lipid composition of the ciliary membrane is deregulated, the ciliary receptors are also deregulated, which can lead to a deregulation of several signalling pathways such as *Shh* [22,23,29–32].

Regarding the axoneme, it is made up of 9 doublets of highly stable microtubules, being more dynamic at the ciliary tip and essential for maintaining the integrity of the cilium[21]. The microtubules are composed of α-tubulin and β-tubulin and are maintained thanks to posttranslational modifications (PTMs) of tubulin called "tubulin code"[21,33]. The integrity of the cilium is maintained due to the proteins responsible for transporting molecules in a bidirectional direction along the cilium, the intraflagellar transport proteins (IFT), which move between the ciliary membrane and the axoneme, the direction of transport depends on two "motors", kinesin-II responsible for anterograde transport (basal body to ciliary tip) and cytoplasmic dynein-2 responsible for retrograde transport (ciliary tip to basal body)[21,34,35].

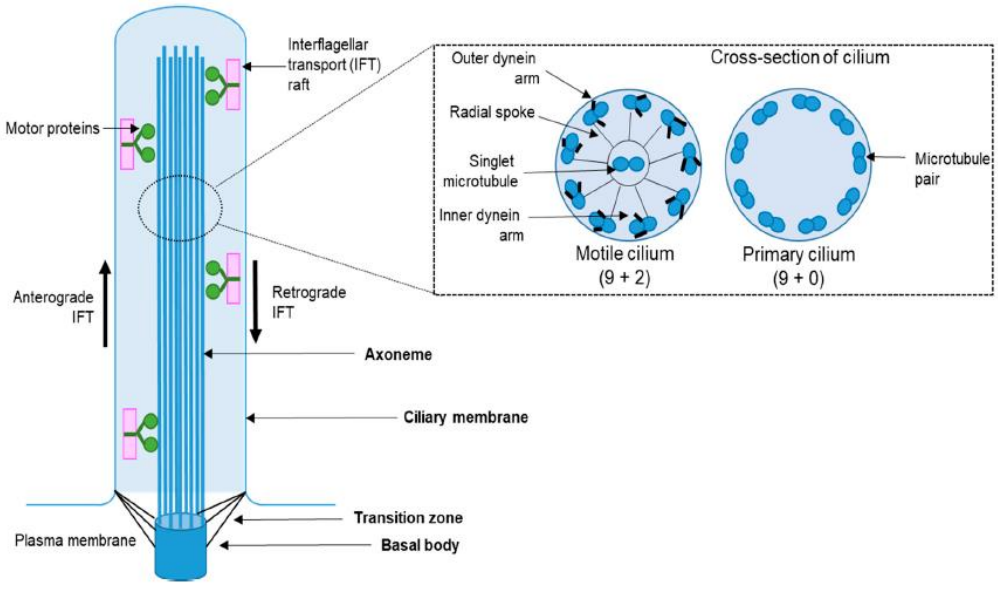

Figure 1.1. Simplified illustration of cilium structure (adaptation from Patel & Tsiokas, 2021)[29]

1.2.2. Tubulin acetylation

Posttranslational modifications, such as acetylation, methylation, deacetylation, and phosphorylation, among others, consist of the removal or addition of chemical group to amino acids[36]. These processes, namely the posttranslational modifications of tubulin, are responsible for maintaining the integrity and stability of the microtubules of the ciliary axoneme, consisting of α-tubulin and β-tubulin[27].

Acetylation of α-tubulin at Lys40 (K20) is the most prevalent acetylation event in the cilium and is catalysed by the enzyme α-tubulin acetyltransferase (ATAT1)[36]. This process occurs in the lumen of the axoneme microtubules and is distributed uniformly throughout the axoneme, both in the central and surrounding microtubules[36]. Acetylation consists of the addition of an acetyl group to a given amino acid, being the acetylation at Lys40 of α-tubulin (K20) essential for the construction of the primary cilium[36,37]. The acetylation of α-tubulin at Lys40 is reversible through deacetylation, which promotes the disassembly of the primary cilium[27]. This mechanism is mediated by the enzymes histone deacetylase 6 (HDAC6) and sirtuin type 2 deacetylase (SIRT2), highly enriched in cilia; when these enzymes are deregulated, the length of the cilium changes; for instance, if the enzymes HDAC6 and SIRT2 are not present, the size of the primary cilium increases, whereas if such enzymes are overexpressed the cilia become shorter [27,33,37,38].

Currently, the relationship between acetylated α-tubulin and ciliary structure/function is still unknown, but over the past few years, several studies have demonstrated that acetylated α-tubulin is essential in cilium assembly and maintenance of its stability[36,37,39]. On the other hand, it is known that in several ciliopathies, an alteration in the α-tubulin acetylation process leads to ciliary malformation[36,38].

1.2.3. Ciliary vesicles

Extracellular vesicles are structures delimited by lipid bilayers that are secreted from the cell surface into the extracellular environment that, are filled up with proteins, lipid, and non-coding RNAs, and which, play a fundamental role in cellular communication[40]. There are two groups of extracellular vesicles: the large ones, also known as ectosomes, formed from budding from the plasma membrane, and the small ones, known as exosomes, formed within multivesicular bodies[41].

In recent years, ciliary vesicles, from the ectosome type, have been identified throughout the cilium, namely in the ciliary tip, in the ciliary membrane and in the ciliary base[41]. These structures are derived from the ciliary membrane but have a different protein composition and are enriched in proteases, small GTPases and ubiquitinated proteins[31,42]. Considering the size and how these structures are secreted, they were called ciliary ectosomes[31,41]. These ectosomes are fundamental in intercellular communication, in controlling the size of the cilia through the incorporation or elimination of substances present in the ciliary membrane, and in maintaining the homeostasis of the ciliary membrane; however, it is not yet known exactly how these processes occur[41,43–45].

1.2.4. Relationship between the primary cilium and sphingolipids

Although it is not yet fully known how the ciliary lipid membrane interacts with ciliary proteins to maintain ciliary integrity, it is known that since the ciliary membrane is made up of glycosphingolipids and ceramide and presents essential transmembrane receptors along the cilium for ciliary signalling, this signalling depends on the correct lipid composition of the ciliary membrane[22,35]. Intraflagellar transport

proteins together with lipids, especially ceramide, are fundamental in the maintenance of the cilium and for correct ciliogenesis, as the expansion and maintenance of the ciliary membrane depends on correct lipid transport regulated by vesicular transport and fusion[46]. Previous studies have demonstrated that ceramide is essential for ciliogenesis, as it regulates the process of α-tubulin acetylation through its interaction with the HDAC6 enzyme[35,46].

In addition to the relationship between ceramide and ciliogenesis, it has recently been found that ceramide also plays an important role in intraflagellar transport, promoting IFT mobility[35]. It is known that intraflagellar transport proteins move along the cilium between the ciliary membrane and the axoneme, but the association between the axoneme and the membrane remains unclear[35]. Currently, some believe that this association is mediated by ceramide as previous studies have shown that ceramide binds to IFTs, forming a connection between the ciliary membrane and the axonema[35]. When ceramide is not present, microtubule organization is disrupted, pointing that ceramide seems essential for maintaining ciliary integrity[35].

1.3. Hedgehog pathway

The Hedgehog (*Hh*) signalling pathway is a major player both in vertebrates and invertebrates during embryonic development, namely for organogenesis, regeneration, and homeostasis, with three ligands described until date: Sonic Hedgehog (*Shh*), Indian Hedgehog (*Ihh*) and Desert Hedgehog (*Dhh*)[47,48].

1.3.1. Sonic hedgehog pathway (*Shh)*

The *Shh* pathway is one of the most studied signalling pathway and consists of 4 main elements: (1) a ligand, (2) the twelve-pass transmembrane receptor Patched1 (Ptch1), (3) the seven-pass transmembrane G protein-coupled receptor Smoothened (Smo) and (4) the transcription factors Gli[49]. It is important to highlight that in vertebrates, all these elements are highly enriched in the primary cilium, causing the entire *Shh* signalling pathway to occur within the primary cilium, making this organelle essential for the activation of the pathway[24,50]. There are two forms of activation of the *Shh* pathway: by canonical signalling which depends on the binding of the ligand (*Shh*) to Ptch1, or by a non-canonical signalling where the pathway is activated downstream of the smoothened receptor[47,51].

When the *Shh* pathway is not activated (Fig.1.2A), Ptch1 inhibits the Smo protein, which is responsible for controlling the activity of Gli transcription factors. There are three Gli proteins, Gli1 that functions only as a transcription activator and Gli2 and Gli3, which function as activators (GliA) or as repressors (GliR) of transcription; the switch between the repressive and activating forms occurs through post-translational modifications and is dependent on the *Shh* protein[46,47,52,53]. Thus, in the absence of the *Shh* ligand, the Gli2 and Gli3 are bound to the suppressor of Fused (SUFU); with the help of intraflagellar transport proteins, the Gli/SUFU protein complexes are transported to the ciliary tip, where Gli2/3 phosphorylation mediated by the proteins kinase A (PKA), casein kinase 1 (CK1) and glycogen synthase kinase 3β (GSK3β) leads to their dissociation from the protein complex and further GliR2/3 [53–55]. GliR2/3 then translocate to the nucleus where they act as transcriptional repressors of a subset of genes, such as *GLI1* and *PTCH1*, which are essential for Shh activation [53–55].

Activation of *Shh* canonical signalling pathway (Fig.1.2B) is a highly organized sequence of molecular events that occurs in response to the binding of the Sonic Hedgehog protein to its

receptor[23,47,51,53–55]. When *Shh* binds to Ptch1, it is internalized into the cytoplasm where it ends up being degraded in the lysosome; as a result, Smo is no longer inhibited, which leads to an accumulation of Smo in the ciliary membrane, causing its activation [23,47,51,53–55]. When Smo is activated, a cascade of molecular events begins with the dissociation of the SUFU-Gli complexes present in the ciliary tip; further intraflagellar transport of Gli2/3 proteins to the base of the cilium and their translocation into the nucleus allow transcription activation of *Shh* target genes[23,47,51,53–55].

Regarding the non-canonical *Shh* signalling pathway, this is a less understood and more complex signalling pathway and may therefore involve different alternative signalling pathways, which do not require all the players of the canonical one (*Shh*-Ptch1-Smo-Gli) [47,54]. It occurs independently of Gli proteins and can occur in two distinct ways: (1) downstream of Smo, causing changes in the levels of calcium and actin present in the cytoskeleton, which have recently been discovered to be associated to the acetylation of α-tubulin in the primary cilium, and (2) independent of Smo, which leads to an increase in cell proliferation [47,54]. Changes in this signalling pathway are related to the formation and progression of some types of cancer [47,54].

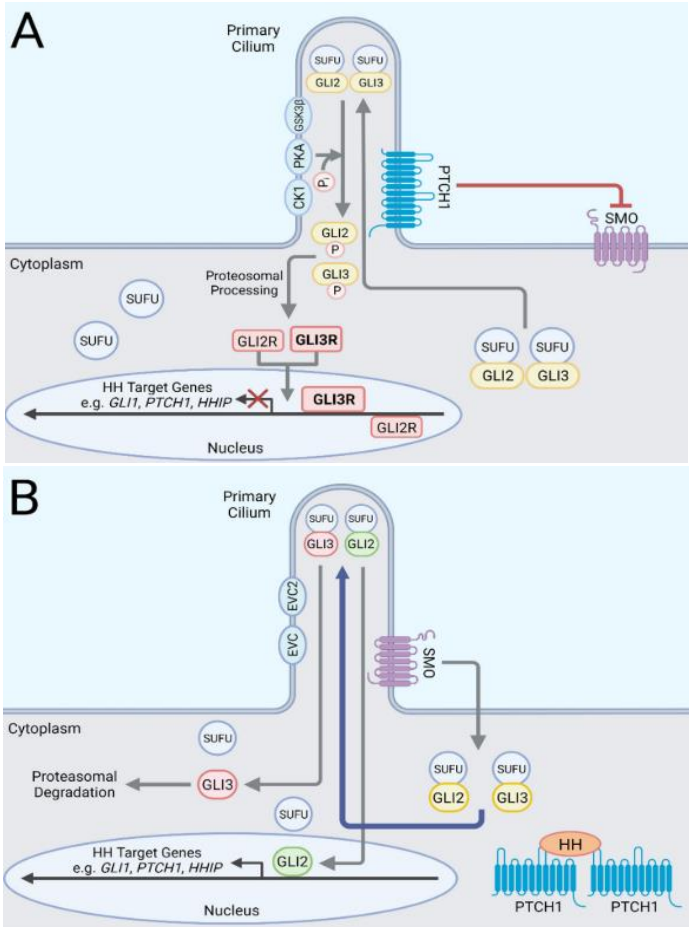

Figure 1.2. Illustration of the canonical *Shh* signalling pathway. (A) Without *Shh* binding to Ptch1, the pathway is not activated. (B) Activation of the *Shh* pathway through binding of *Shh* to Ptch1. (Adapted from Suchors & Kim, 2022) [51]

1.4. Alternative splicing

Splicing is the process through which the removal of introns (noncoding sequences) and the ligation of exons (coding sequence) occurs, leading to the maturation of pre-mRNA into mRNA which is made up only of coding sequences; this process occurs through the spliceosome complex consisting of five small nuclear ribonucleoprotein particles (snRNPs, U1, U2, U4-U6) that contain small nuclear RNAs (snRNAs) responsible for identifying the splice sites present in the pre-mRNAs[56–59]. Notice that a major step in splicing regulation involves identifying the 5' and 3' splice sites that determine the beginning and end of the intron, respectively[60].

During this process, while some exons, the so-called constitutive exons, are always included in the mature mRNA, others, the so-called alternative exons, may or may not be included, in a phenomenon called alternative splicing[56]. It is estimated that this alternative splicing mechanism, where certain exons present in the pre-mRNA may or may not be included in the final mRNA, occurs in > 90% of human transcripts, leading to the formation of mRNAs that will encode different isoforms of the initial protein, being the main mechanism responsible for the enormous diversity in our proteome[56]. As illustrated in Figure 1.3, the alternative splicing mechanism can occur in several ways namely: (1) exon skipping that is the most common event in which an exon is excluded; (2) intron retention, where one of the introns remains present in the mature mRNA; (3) alternative 5’ or 3’ splice site, where spliceosome must “choose” between 2 or more splice sites present in exon/intron boundary; and (4) mutually exclusive exons, in which only one of two exons is included in the mature mRNA isoform[61–63].

Changes in the regulation of splicing events are associated with a variety of genetic diseases, including lysosomal disorders; therefore studies have been carried out to develop therapies that can reverse the effect caused by changes in splicing events [57,59,64,65]. Currently, the most promising therapy involves the use of antisense oligonucleotides (ASOs), which are nucleic acid polymers capable of masking a specific sequence of a target transcript, modulating alternative splicing events through the exclusion or inclusion of specific exons (exon skipping and intron retention)[57,59,64,65].

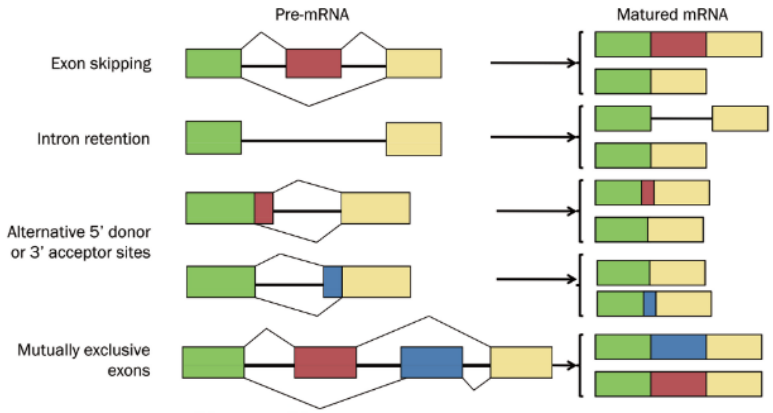

Figure 1.3. Simplified illustration of alternative splicing events: exon skipping, intron retention, alternative 5’ or 3’ splice site and mutually exclusive exons. (Adapted from Le et al., 2015) [61]

1.6. Objectives

The present study was performed in the laboratory of Prof.ª Dr.ª Maria Carmo-Fonseca in order to understand which changes in genetic expression are associated with Gaucher disease, namely the impact of mis-splicing in the appearance and progression of this disorder. Previously, in the laboratory the primary fibroblasts of three individuals with Gaucher disease and the primary fibroblasts of three apparently healthy individuals (control) were analysed by RNA-seq; after bioinformatic analysis of these data, alterations in the alternative splicing pattern of a subset of ciliary genes were found. With the aim of clarifying the relationship between primary cilia and Gaucher disease, a partnership was created between the group of Prof.ª Dr.ª Maria Carmo-Fonseca from the Institute of Molecular Medicine and the group of Prof.ª Dr.ª Susana Lopes da Nova Medical School Research. Therefore, this project has three main objectives:

1) Validation by qRT-PCR of differential alternative splicing events, previously detected by RNA-seq, in ciliary genes of Gaucher and healthy primary human fibroblasts;
2) Morphological characterisation of the primary cilium of fibroblasts from individuals with Gaucher's disease in comparison with fibroblasts derived from healthy cells;
3) Functional evaluation of the Shh signal transduction pathway associated with the primary cilium and the expression levels of intraflagellar transport proteins, in fibroblasts from healthy *versus* Gaucher individuals.

Chapter 2. Materials and Methods

2.1. Cell Lines

In this project, primary human fibroblast cultures were used, which were acquired at the "Coriell Institute for Medical Research". Four cell lines from apparently healthy individuals (WT cell lines) and four cell lines from individuals with Gaucher disease, an autosomal recessive disease (Gaucher cell lines) were analysed, namely: GM00498, GM05565, GM07522, GM00323, GM02627, GM00852, GM07968 and GM020270.

2.1.1. Characterization of WT cell lines

All WT cell lines were obtained from skin biopsies of apparently healthy donors. Both GM0498 and GM05565 derived from 3-year-old male children, the last one of latin ascendency. GM07522 was obtained from a 19-year-old female, whereas GM00323 derived from an 11-year-old-male.

2.1.2. Characterization of Gaucher cell lines

All Gaucher cell lines carry a specific, pathogenic mutation on chromosome 1q21 in the *GBA1* gene that leads to Gaucher disease. To have a greater representation of the disease under study, 2 cell lines from individuals with type I of Gaucher disease (GM00853 and GM7968) and 2 lines from individuals with type II (GM02627 and GM020270) were used.

Regarding the lines from donors with Gaucher type I, GM00852 cell line derived from a 20-year-old male patient, who has an A370S mutation that leads to residual β-Glucocerebrosidase enzymatic activity (6%). On the other hand, the GM07968 cell line was obtained from a biopsy performed on a 19-week-old male foetus, descended from a Jewish family, and has a L483P mutation with a unknow level of reduction in enzymatic activity.

In terms of cell lines from individuals with type II Gaucher disease, GM02627 cell line derived from a 3-year-old female and is characterized by the G325R mutation that leads to an enzymatic activity reduction of 24%. GM020270 cell line comes from a female donor of African/Felipino ethnicity with only 4 months of age, which carries a L483P mutation with a unknow level of reduction in enzymatic activity.

2.2. Cell Culture

During this project, five study groups were analysed: (1) a first study group, consisting of four primary fibroblast cell lines obtained from apparently healthy individuals, control study group; (2) a second study group, this one consisting of four primary fibroblast cell lines obtained from 4 individuals with Gaucher disease (with subtypes I and II), Gaucher study group; (3) a third group that consisted in the same primary Gaucher fibroblast lines treated with recombinant GBA (Gcase) for 5 days, Gaucher + Gcase study group; (4) a fourth group aiming to analyse the potential involvement of the Sonic Hedgehog (*Shh*) signaling pathway into Gaucher disease, for which the Smoothened agonist (SAG) was added for 24h to WT and Gaucher fibroblast cell lines, study group WT + SAG and Gaucher + SAG;

(5) and, finally, the last group, which aimed to investigate whether treatment of Gaucher fibroblasts with Gcase impacted the *Shh* signaling pathway, and where for this purpose Gaucher cell lines were treated with Gcase for 5 days and SAG was added in the last 24h of Gcase treatment, study group Gaucher + Gcase + SAG.

All primary fibroblasts cell lines were cultured in Minimum Essential Medium (MEM) supplemented with 15% FBS (Fetal Bovine Serum) and 1% L-Glutamin, kept in 25 cm^2 flasks (T25) and placed in an incubator at 37ºC, in an environment with 5% CO_2.

The experiments were carried out in 6-well plates, with 2 coverslips added to each of the wells to process cells for further morphological analysis. Briefly, T25 flasks of fully confluent cells were trypsinized in 2 ml of 0.25% Trypsin-EDTA and placed for 3 minutes in the incubator at 37°C. Then, after shaking to detach all cells from the bottom of the flasks, cells were resuspended into 3 ml of MEM and 0.5 ml of cell suspension was transferred to each 6-well plate. 1 ml of MEM were further added to each well, up to a final volume of 1.5ml/well. 48 hours after cells reached approximately 80% confluency, to stimulate the development of cilia, cells were placed in starvation for an additional 72h. To do so fibroblasts were washed three times with 1xPBS to remove all the FBS present in the previous medium. After the washes, 1.5 ml of MEM supplemented only with 1% L-Glutamin was added to each 6-well dish.

2.2.1. Treatment with SAG

To study the potential involvement of the Sonic Hedgehog signaling pathway into Gaucher disease, the Smoothened agonist was added for 24h before collection of the cells. To do so, two days after reaching approximately 80% confluency, starvation was induced as previously described. Then, when cells were starved for 48h, 0.8 µl/ml of SAG was added to the respective 6 well plate and kept for an additional 24h.

After 72 hours of starvation and 24 hours of SAG treatment (day 5 of experiment), cells that were grown on coverslips were fixed in 3.7% PFA /1xPBS and the remaining cells of the dish were subjected to the RNA extraction protocol.

2.2.2. Treatment with Gcase

The Gcase used in this project, was the Imiglucerase produced by the Genzyme laboratory, known commercially as Cerezyme. This medication was provided by the Clinical Trials department of Hospital Santa Maria where the whole process of preparing the drug was taken care of by the department's team.

As previously mentioned, the experiments were carried out in 6-well plates. After the cells reached approximately 80% of confluency, 5-day experiments were started by the addition of 6.5 µl/ml of Imiglucerase (0.26U/ml) to Gaucher cells. Two days after Gcase addition, starvation was initiated for an additional 72 hours. For the SAG study group, 0.8 µl/ml of SAG were added 24h before cells were collected. Cell culture medium and enzyme were replaced every 48 hours.

After 5 days of Gcase treatment and 72 hours of starvation (and for the SAG study group, 24 hours of SAG treatment) (day 5 of experiment), cells that were grown on coverslips were fixed in 3.7% PFA /1xPBS and the remaining cells of the dish were subjected to the RNA extraction protocol.

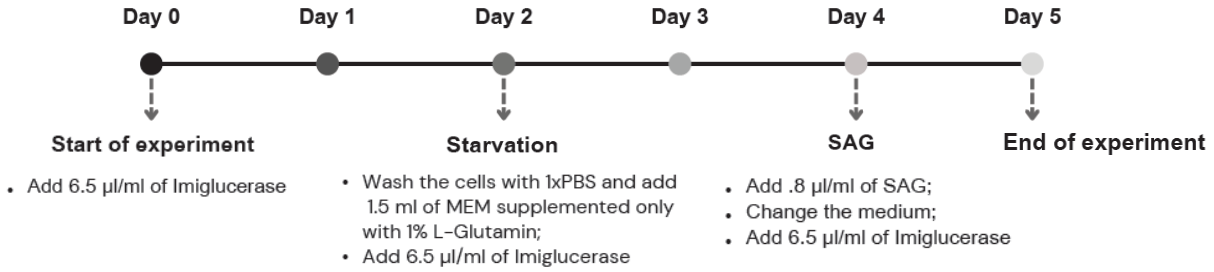

Figure 2.1. Timeline of treatment of the experimental design.

2.3. Morphological analysis of primary cilia

2.3.1. Immunohistochemistry

For cilia morphology studies, cells from each experimental group were subjected to a quick wash with 1x PBS and were fixed for 10 minutes in 3.7% PFA /1xPBS. Cells were then washed with 0.05% Tween in PBS and permeabilized for 5 minutes in 1xPBS/0.5% Tx-100 (0.5% Triton X100) at room temperature (RT).

After the cells were fixed and permeabilized, they were submitted to an immunofluorescence protocol to detect primary cilia. For this, 10 µl of blocking solution (1%FBS in 1xPBS) was added to each coverslip for 30 minutes at RT. Then, 5 µl of each primary antibody, previously diluted in 1%FBS in 1xPBS, were added and left to incubate for 1 hour at 37°C inside a humid box (1 hour for each antibody). Depending on the analysis performed, two pairs of primary antibodies were used: anti-Arl13b and anti-gamma tubulin, which marked the ciliary membrane and basal body, respectively, and anti-Arl13b and anti-Acetylated alpha Tubulin, which was used for marking of the ciliary axoneme. After the primary antibody incubation, cells were briefly washed with 0.05% Tween/1xPBS. Subsequently, 5 µl of secondary antibody was applied and incubated inside a light-protected box for 1 hour at room temperature. Nuclei were stained by adding 10 µl of 4′,6-diamidino-2-phenylindole (DAPI, 1 µg/ µl) in 1xPBS solution for 20 minutes at RT. At the end of the DAPI incubation period, cells were washed twice with 0.05% Tween in 1xPBS and twice with 1xPBS. Finally, cells were mounted on slides using the vectashield vibrance mounting medium and stored at 4°C.

Table I. Table of primary and secondary antibodies used for immunofluorescence assays, previously diluted in 1%FBS in 1xPBS.

Molecule	Primary Antibody	Secondary Antibody
Arl13b	anti-Arl13b (Rabbit) final dilution 1/50	anti-Rabbit-DL495 final dilution 1/200
Gamma Tubulin	anti-gamma-tubulin (Mouse) final dilution 1/100	anti-Mouse-A488 final dilution 1/200
Acetylated alpha Tubulin	anti-Acetylated alpha Tubulin (Mouse) final dilution 1/100	

2.3.2. Microscopy and Image Analysis

The microscope chosen to acquire immunofluorescence cell images was a confocal point-scanning microscope (Zeiss LSM 710), in which a 63x objective with a 0.6x and 2x amplification was used. To be able to carry out the morphological analysis of cilia, the images were obtained along the Z axis (Z-Stack) with a stack spacing of 0.20 µm. Then, the acquired images were collapsed to maximum intensity projections to visualise, in a single image, the different phenotypes observed.

After acquiring the images, the Z-stacks were analysed in ImageJ-Fiji. To quantify the ciliary length, an ImageJ-Fiji framework, the simple neurite tracer (SNT), was used. This Plugin allowed, through the ARL13b staining, to trace the ciliary membrane and subsequently obtain the exact length of each cilia analysed in 3D.

2.3.3. Statistical analysis

The data acquired, from the morphological analysis, were inserted into the GraphPad Prisma 8. Then, to verify whether there were statistically significant differences between the various groups under study, a one-way ANOVA statistical test was performed.

2.4. Molecular Biology assays

2.4.1. RNA extraction

Cells from each study group were subjected to RNA extraction protocol. Briefly, cells were lysed after resuspension in 1 ml of NYZol. Cell lysates were transferred into previously labelled 1.5 ml eppendorfs and left to incubate at RT for 5 minutes with rotation. At the end of 5 minutes, 200 µl of chloroform was added to each eppendorf, the lysates homogenised, and left to incubate for 3 minutes at RT. Aiming to separate the organic phase, consisting of lipids and the majority of genomic DNA, from the aqueous phase containing the RNA, centrifugation was performed at 11900 rpm at 4ºC for 15 minutes. Subsequently, the aqueous phase was carefully transferred to a new eppendorf, in which 650 µl of isopropanol was added, vigorously shake, and left to incubate for 10 minutes at RT. To obtain a clearly visible RNA pellet, 1.5 µl of Glycoblue was added to the solution and placed in the centrifuge for 10 minutes at 11900 rpm at 4°C. Then, the supernatant was discarded and, the RNA pellet, washed with 1 ml of 75% EtOH (RNase, DNase-free H2O prepared), followed by a centrifugation for 10 minutes at 7500 rpm at 4°C. With great caution, the supernatant was again discarded, and the RNA pellet was left to air dry for at least 10 minutes. When the pellet was completely dry, it was resuspended in 13 µl of RNase-free water and RNA quantified in the Nanodrop.

To avoid any DNA contamination, 1 to 5 µl of RNA, depending on the quantification obtained in the Nanodrop, 5 µl of 10x DNase I buffer, 3 µl of DNase I and 1 µl of Ribosafe were mixed in a new Eppendorf into a final volume of 50 µl, and left to incubate for 2 hours at 37°C. After the incubation period, for each 50 µl of reaction, 0.1V of 3M AcNa (5 µl), 3V of 100% EtOH (150 µl) and 1 µl of Glycogen Blue were added and RNA was allowed to precipitate overnight at -20ºC. Subsequently, a spin max speed (>13000 rpm) was performed at 4ºC for 30 minutes, the supernatant was discarded, the pellet was washed with 75 µl of 75% EtOH and subjected to a vortex and spin max speed at 4ºC for 15 minutes. Finally, the supernatant was again discarded, and the pellet was left to air dry for at least 10 minutes. RNA was resuspended in 13 µl of RNase-free water and quantified once more time in the Nanodrop.

2.4.2. cDNA synthesis

After the RNA extraction protocol, the cDNA synthesis protocol was performed. In each 200 µl PCR Eppendorf tube, 1000 ng of RNA, 2 µl of random primers and RNase-free water was added, up to a final volume of 11.4 µl. After a brief spin, samples were placed in the thermocycler for 10 minutes at 65°C, to prevent RNA secondary structures. Then, after cooling, 8.6 µl of a reverse transcriptase mix was added to each eppendorf, containing 4 µl of 5x RT buffer, 0.5 µl of RNase OUT (40 U/ µl) responsible for maintaining RNA integrity, 2 µl of 10 mM dNTP mix, 1 µl of 0.1 M DTT that maintains enzymatic activity and 1.1 µl of reverse transcriptase.

Reactions were incubated for 10 minutes at 29°C to allow primers annealing, followed by an incubation period of 60 minutes at 48°C where DNA polymerization occurred and finally for 5 minutes at 85°C where the enzyme was deactivated and RNA templates degraded. At the end, samples were removed from the thermocycler and the cDNAs were stored at -20°C until further use.

2.4.3. Real-Time Quantitative Reverse Transcription Polymerase Chain Reaction (qRT – PCR)

Two different assays were used of real-time quantitative reverse transcription polymerase chain reaction (qRT-PCR) were performed: a first one, using the SYBR green reagent, for the analysis of expression and alternative splicing events of ciliary genes and, a second one, using highly specific TaqMan probes, for assessment of activation of the *Shh* signalling pathway, under the experimental conditions used.

Using the SYBR green assay, 6 alternative splicing events in 6 different ciliary genes, previously identified by RNA sequencing as being distinct in WT versus Gaucher fibroblasts, were selected and analysed using the following pairs of primers: (1) AKNA AFE (alternative first exon) inclusion against total AKNA Ex3; (2) TTC23 Ex3 inclusion against total TTC23 Ex5; (3) IFT88 Ex6 inclusion, normalised against total Ex17; (4) CDK20 Ex5 inclusion, normalised against total CDK20 Ex3; (5) IFT122 Ex18 inclusion, normalised against total IFT122 Ex26; (6) OFD1 Ex19 inclusion, normalised against total OFD1 Ex14. Alternative splicing events were analysed using primers specific for the exon to be included. For primer sequence details, see Supplementary Table II.

To do so, a qRT-PCR mix was prepared for each pair of primers, where 6 µl of SYBR green Master Mix (BioRad), 0.5 µl of 10 µM forward primer and 0.5 µl of 10 µM reverse primer were added per reaction. Subsequently, a 384-well plate was prepared in which each of the samples under study was run in triplicate. In each well, 5 µl of previously diluted cDNA (1:15) and 7 µl of the respective qRT-PCR mix were added.

Using specific TaqMan probes assay (Applied Biosystems), expression of two major genes, *PTCH1* and *GLI1* of the *Shh* signalling pathway was analysed, upon normalisation against the housekeeping *HPRT1* gene. To do so, a qRT-PCR mix was prepared for each TaqMan probe, where per reaction 5 µl of Master Mix (2x) and 0.5 µl of TaqMan gene Expression probe (20x) were added. 384-well plates were set up by adding 5.5 µl of qRT-PCR mix and 5 µl of previously diluted cDNA (1:6) into each well, up to a final volume of 10.5 µl. Each of the samples under study was run in triplicate.

384-well plates were subjected to a spin at 700g for 3 minutes and run in the ViiA 7 Real-Time PCR System machine, using standard amplification protocols for each of the assays.

Chapter 3. Results

3.1. Morphological analysis of the primary cilium

To analyse the morphology of primary cilia, the ciliary membrane and the basal body were immunofluorescently stained using anti-Arl13b and anti-gamma tubulin antibodies, respectively. This analysis was performed for the five experimental groups: WT, Gaucher, Gaucher + Gcase, Gaucher + SAG and Gaucher + Gcase + SAG. Arl13b is a member of the ARF family of regulatory GTPases and is highly enriched in the ciliary membrane[49,66]. This protein plays a fundamental role in the process of formation and maintenance of the cilium through the regulation of intraflagellar transport and the phospholipid composition of the ciliary membrane through the recruitment of Inositol Polyphosphate-5-Phosphatase E (INPP5E) responsible for the correct maintenance of PtdIns4P to the ciliary membrane on the other hand, it participates in the regulation of Hedgehog signaling and endocytic trafficking[32,49,66].

Comparing the ciliary length of WT and Gaucher cilia, there was a significant increase in the length of the cilia in Gaucher samples (Fig.3.3A, ρ-value < 0.001). On the other hand, when the Gaucher + Gcase experimental group was analysed, a rescue of the ciliary length phenotype was observed (ρ-value < 0.0001), thus making the length of these cilia closer to the values observed in WT (Fig.3.3B). Regarding the Gaucher + SAG and Gaucher + Gcase + SAG study groups, there were no statistically significant differences in ciliary length compared to the WT and Gaucher groups (Fig.3.3C).

In the Gaucher group, in addition to the increase in ciliary length, it was also possible to observe the appearance of cilia with an intermittent Arl13b staining (Fig.3.1E), this phenotype may be indicative of the existence of alterations in the membrane composition or in the internal structure of the cilium, namely in the axoneme. However, here, when the Gaucher + Gcase experimental group was analysed, in contrary to the rescue observed in the ciliary length, the cilia continued to present an intermittent Arl13b staining (Fig.3.1C). Also, in the Gaucher + SAG and Gaucher + Gcase + SAG study groups, the Arl13b staining remained intermittent, as observed in many cilia of fibroblasts from Gaucher patients (Fig.3.2).

From these experiments overall, we observe an increase in the ciliary length in Gaucher cells compared to the WT ones, with an intermittent Arl13b staining phenotype being frequent in the Gaucher group. On the other hand, after Gcase treatment during 5 days, it was only possible to rescue the ciliary length of Gaucher cells to normal WT values, with the cilia of such cells continuing to show an intermittent phenotype in their Arl13b staining that was not rescued after Gcase treatment.

To verify whether the intermittent Arl13b staining observed in Gaucher cilia, resulted from alterations in the internal structure of the primary cilium, the axoneme and the membrane were immunofluorescent co-stained using anti-acetylated alpha tubulin and anti-Arl13b antibodies, respectively (Fig.3.1G-L). This experiment was carried out in the WT, Gaucher and Gaucher + Gcase experimental groups.

Comparing the Arl13b and acetylated alpha tubulin immunofluorescence stainings, it was possible to identify four phenotypes, illustrated in Figure 3.4D : (1) continuous Arl13b staining, with both proteins being present up to the ciliary tip (Fig.3.1G); (2) continuous Arl13b staining, but the labelling does not coincide up to the ciliary tip, which means that the acetylated alpha tubulin does not extend to the tip of the cilia (Fig.3.1L); (3) intermittent Arl13b staining, with both proteins being present up to the ciliary tip (Fig.3.1H); (4) the last observed phenotype presents intermittent Arl13b staining without colocalization of both proteins up to the ciliary tip (Fig.3.1K).

Analysing the WT cilia, it was possible to verify that 95% of the cilia had a continuous Arl13b staining and both labelling were coincident up to the ciliary tip (Fig.3.4A). In the cilia from Gaucher patient fibroblasts (Fig.3.4B), there was a decreased in the frequency of cilia with continuous Arl13b staining and both labelling were coincident up to the ciliary tip (35%) and an increase in the frequency of cilia that, despite having a continuous Arl13b staining, did not show colocalization of both proteins up to the ciliary tip (33%, comparing with 2% in WT cells) and of intermittent Arl13b staining, with colocalization of both proteins up to the ciliary tip (23%). Regarding the experimental group Gaucher + Gcase (Fig.3.4C), compared to Gaucher cilia, there was a slight increase in the frequency of cilia with continuous Arl13b staining and both labelling coincident up to the ciliary tip (49% comparing to 35% in Gaucher cells) and a slight decrease in cilia with continuous Arl13b staining, but the labelling not coincident up to the tip (16%). These changes, in the Gaucher + Gcase experimental group, even if not being statistically significant, show a tendency towards an increase in the frequency of cilia with the "normal" phenotype (continuous Arl13b staining with both labelling being coincident up to the ciliary tip of the cilium) when compared to Gaucher cilia; however, no can be stated that upon Gcase treatment there was a correction of the anomalies observed in the axoneme of the Gaucher cilia.

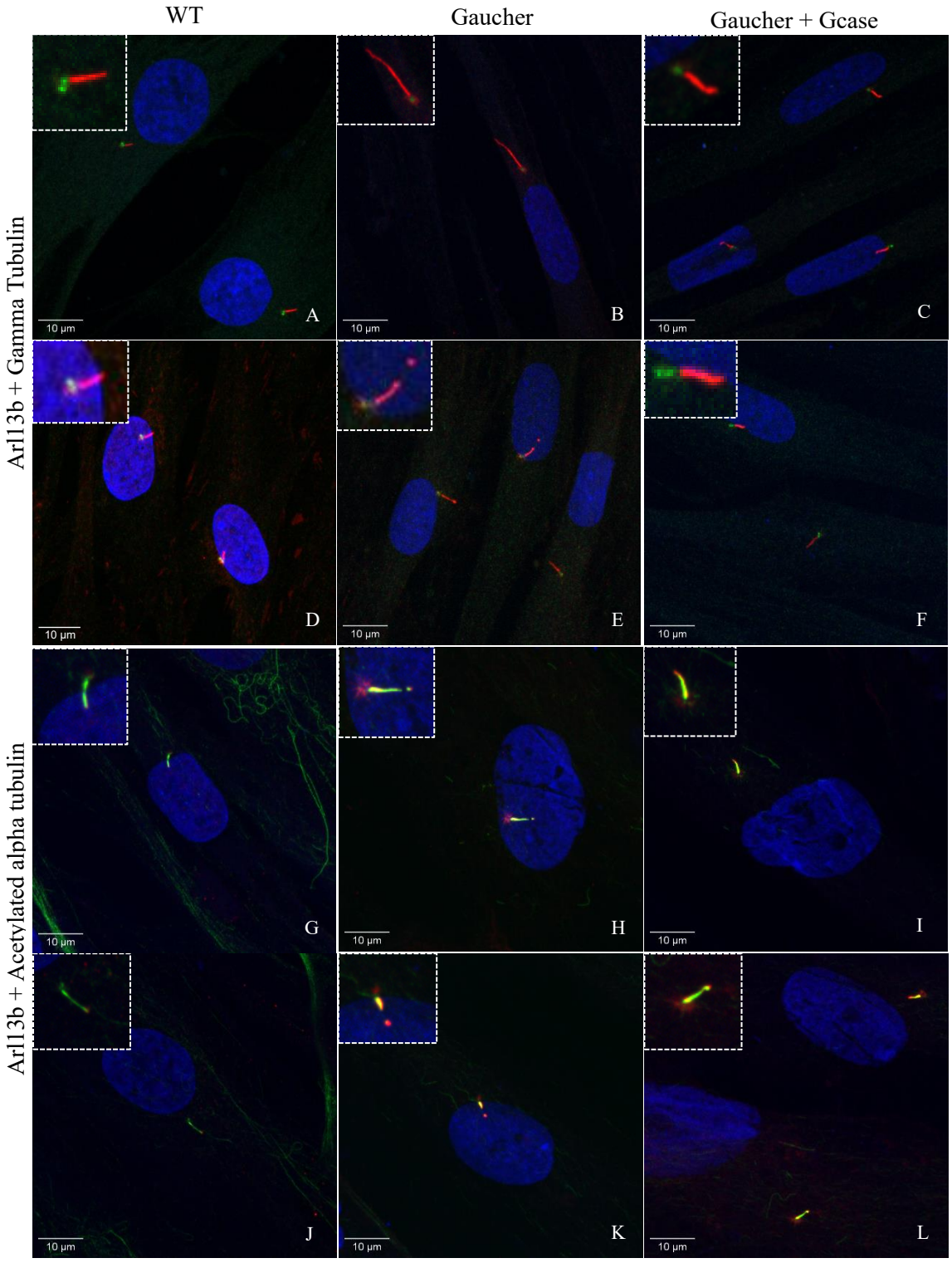

Figure 3.1. (A-L) Representation of the primary cilium through confocal maximum intensity z-projections, obtained through a 63x objective and 2x amplification. The ciliary membrane (in red) was immunofluorescently stained using the primary antibody anti-Arl13b (1/50 dilution) followed by the anti-Rabbit-DL495 (1/200 dilution). Nuclei were labeled with DAPI. Scale bar, 10 µm. **(A-F)** The basal body is represented in green, which was immunofluorescently stained with the primary antibody anti-gamma-tubulin (1/100 dilution) followed by the anti-Mouse-A488 antibody (1/200 dilution). **(G-L)** The ciliary exoneme (green) was immunofluorescently stained with the primary antibody anti-Acetylated alpha tubulin (1/100 dilution) followed by the secondary anti-Mouse antibody-A488 (1/200 dilution). **(A,G and J,** WT GM00323), **(B and C,** Gaucher GM00852), **(D,** WT GM07522), **(E,F,H,I,K and L,** Gaucher GM02627).

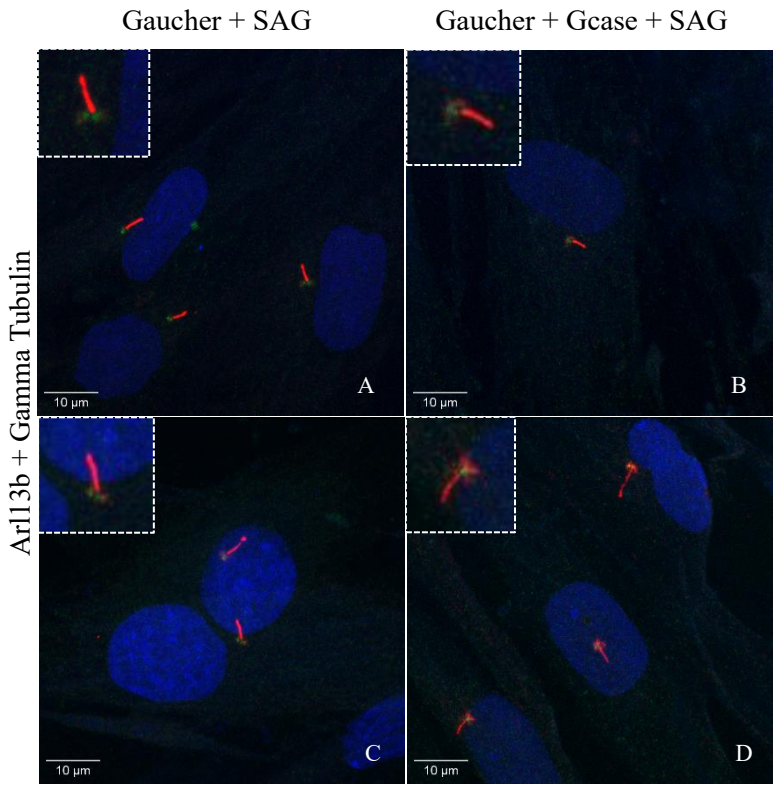

Figure 3.2. (A-D) Representation of the primary cilium through confocal maximum intensity z-projections, obtained with a 63x objective and 2x amplification. The ciliary membrane (in red) was immunofluorescently stained using the primary antibody anti-Arl13b (1/50 dilution) followed by the anti-Rabbit-DL495 (1/200 dilution). Basal body (in green) was immunofluorescently stained with the primary anti-gamma-tubulin (1/100 dilution) followed by the anti-Mouse-A488 (1/200 dilution). Nuclei were labeled with DAPI. Scale bar, 10 µm. **(A-B**, Gaucher GM00852), **(C-D**, Gaucher GM02627).

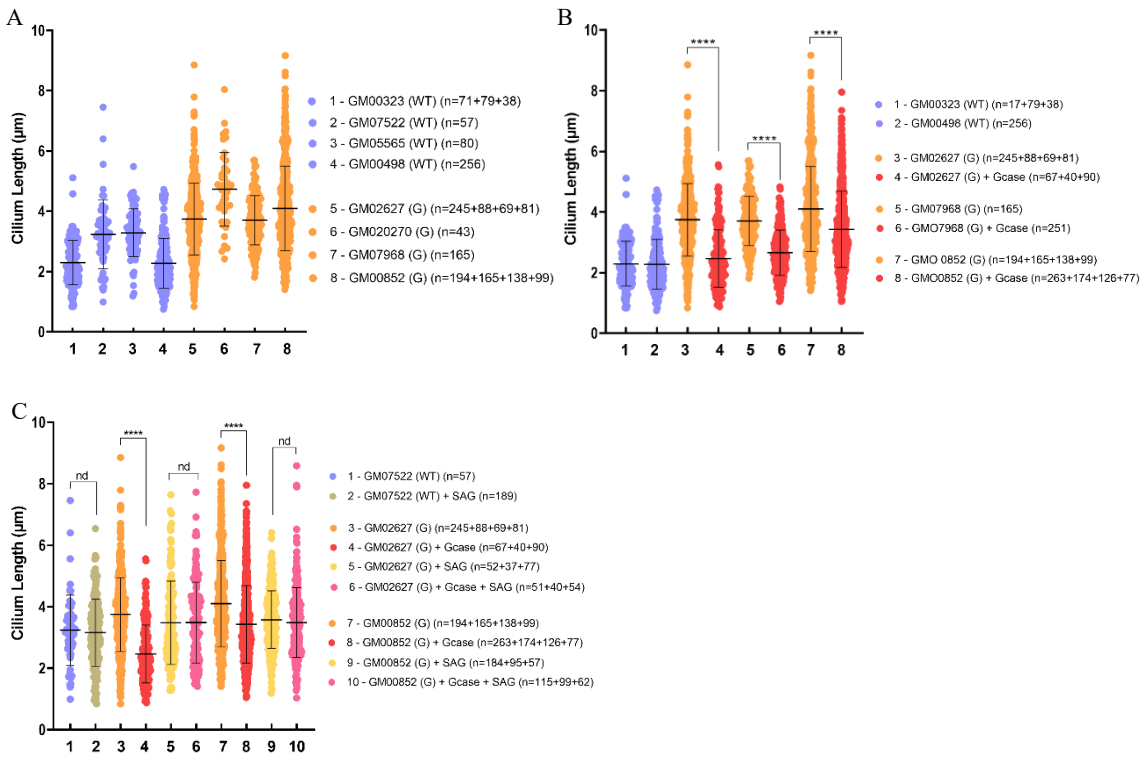

Figure 3.3. (A-C) Analysis of primary cilium length (µm), through Arl13b staining. The number of cilia analyzed in each cell line is represented within parentheses. The sign + separates different replicates. One-way ANOVA test: **** ρ-value < 0.0001. **(A)** Comparison between the WT cell lines (GM00323, GM07522, GM05565 and GM00498, in blue) and the Gaucher cell lines (GM02627, GM020270, GM07968 and GM00852, in orange). **(B)** Comparison between WT cell lines (GM00323 and GM00498, in blue), Gaucher lines (GM02627, GM07968 and GM00852, in orange) and Gaucher lines treated for 5 days with recombinant Gcase (GM02627, GM07968 and GM00852, in red). **(C)** Comparison between study groups WT (GM07522, in blue), WT + SAG (GM07522, in gray), Gaucher (GM02627 and GM00852, in orange), Gaucher + Gcase (GM02627 and GM00852, in red), Gaucher + SAG (GM02627 and GM00852, in yellow) and the last Gaucher + Gcase + SAG group (GM02627 and GM00852, in pink). A one-way ANOVA statistical test was performed between groups. **** ρ-value < 0.0001, nd: not statistically different.

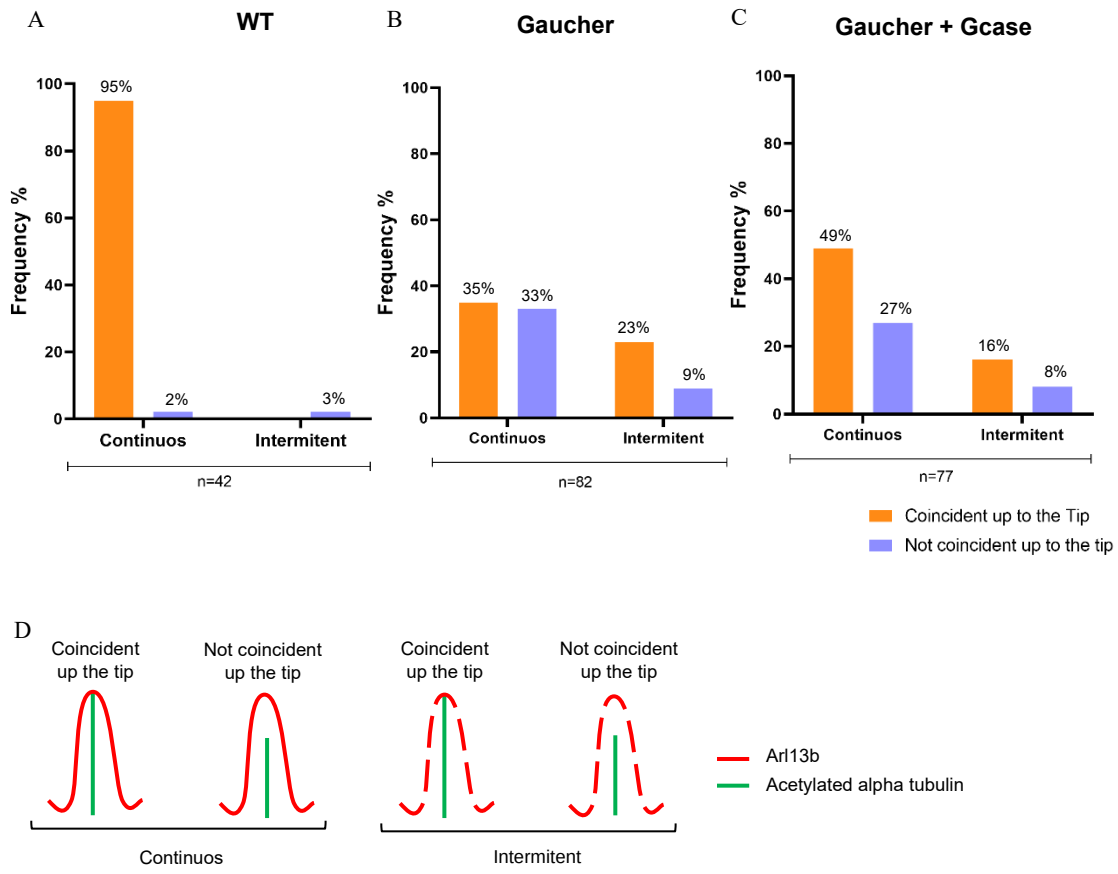

Figure 3.4. (A-C) Percentages of the phenotypes observed in WT **(A),** Gaucher **(B)** and Gaucher + Gcase **(C)** upon Arl13b and acetylated tubulin immunofluorescence double staining. **(D)** Illustration of the four observed phenotypes observed through the co-staining with the anti-acetylated alpha tubulin and Arl13b antibodies.

3.2. Molecular Biology analyses of the primary cilium

3.2.1. Analysis of *Shh* signaling pathway activation

Sonic Hedgehog is a major signaling pathway in vertebrates. To clarify whether, in addition to the morphological differences observed in cilia from Gaucher patients, there were differences in the *Shh* signaling pathway, the expression levels of two major players, the *PTCH1* and *GLI1* genes, were analyzed by qRT-PCR in the WT, Gaucher and Gaucher + Gcase experimental groups. For each experimental group, the following conditions were analyzed: (1) cells that were without starvation for 72 hours; (2) cells that have been in starvation for 72 hours; and finally (3) cells treated with Smoothened agonist (SAG) for 24 hours to induce *Shh* pathways hyperactivation.

Results show that without the addition of SAG, there are no statistical differences in activation of *Shh* signaling pathway among the three experimental groups, with *PTCH1* and *GLI1* expression levels being similar before and after 72h starvation (Fig.3.5A and 3.5B). However, upon SAG treatment, there is a statistically significant increase in the expression levels of both *PTCH1* and *GLI1* genes in Gaucher cells when compared with WT ones, meaning that there is a hyperactivation of the *Shh* signaling pathway in the Gaucher cells that is not reversed upon Gcase treatment for 5 days.

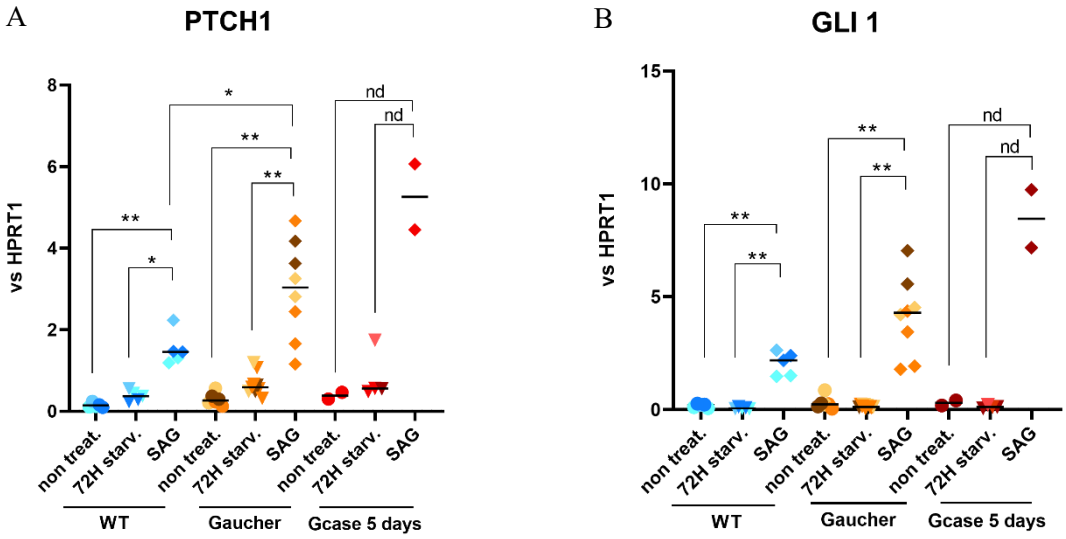

Figure 3.5. Analysis of *PTCH1* **(A)** and *GLI1* **(B)** expression levels genes, normalized against the *HPRT1* housekeeping gene, in the three experimental groups, WT in blue, Gaucher in orange and Gaucher + Gcase in red. Within each experimental group, three different conditions were tested, non-treated fibroblasts that consist of fibroblasts that were not subject to starvation (non treat), fibroblasts placed in starvation for 72h (72H starv) and fibroblasts to which SAG was added for 24h upon 48h of starvation (SAG). A one-way ANOVA statistical test was performed between groups. *ρ-value < 0.5, ** ρ-value < 0.05, nd: non statistical difference.

3.2.2. Analysis of alternative splicing events

Through qRT-PCR, alternative splicing events in six ciliary genes (*AKNE*, *CDK20*, *IFT88*, *IFT122*, *OFD1* and *TTC23*), previously identified by RNA sequencing as being differentially spliced in fibroblasts from Gaucher patients versus fibroblasts from healthy controls, were validated. To do so, pairs of primers were designed to allow specific amplification of transcripts with inclusion of a given exon. Inclusion levels of an alternative splicing exon were inferred upon normalization against the total amount of transcripts present in each sample by using pairs of primers against constitutive exons that were present in all transcripts.

Results confirm that in Gaucher cells, levels of inclusion of a subset of alternatively spliced exons in several ciliary transcripts are statistically different from the ones observed in WT cells; in particular, this was observed for *AKNA*, *OFD1* and *TTC23* transcripts, with lower inclusion of alternative first exon, exon 19 and exon 3, respectively, in Gaucher cells (Fig.3.6A, E, and F, WT in blue, Gaucher in orange), in contrast with inclusion of *IFT122* exon 18, which show higher levels of inclusion in this experimental group (Fig.3.6D, WT in blue, Gaucher in orange). A tendency for lower inclusion of *CDK20* exon 5 and higher inclusion of *IFT88* exon 6 was observed in Gaucher cells when compared with WT ones, despite differences not being statistically significant due to high level of heterogeneity among samples of the same experimental group (Fig.3.6B and C, WT in blue, Gaucher in orange). Upon 5 days of Gcase treatment of Gaucher cells (Fig.3.6, Gcase in red) no significant changes were observed for inclusion of any of the analyzed alternative splicing exons, when compared to the Gaucher experimental group; interestingly, a tendency towards approximation to the values observed in WT group was seen for *CDK20* exon 5, upon Gcase treatment (Fig.3.6B, Gcase in red).

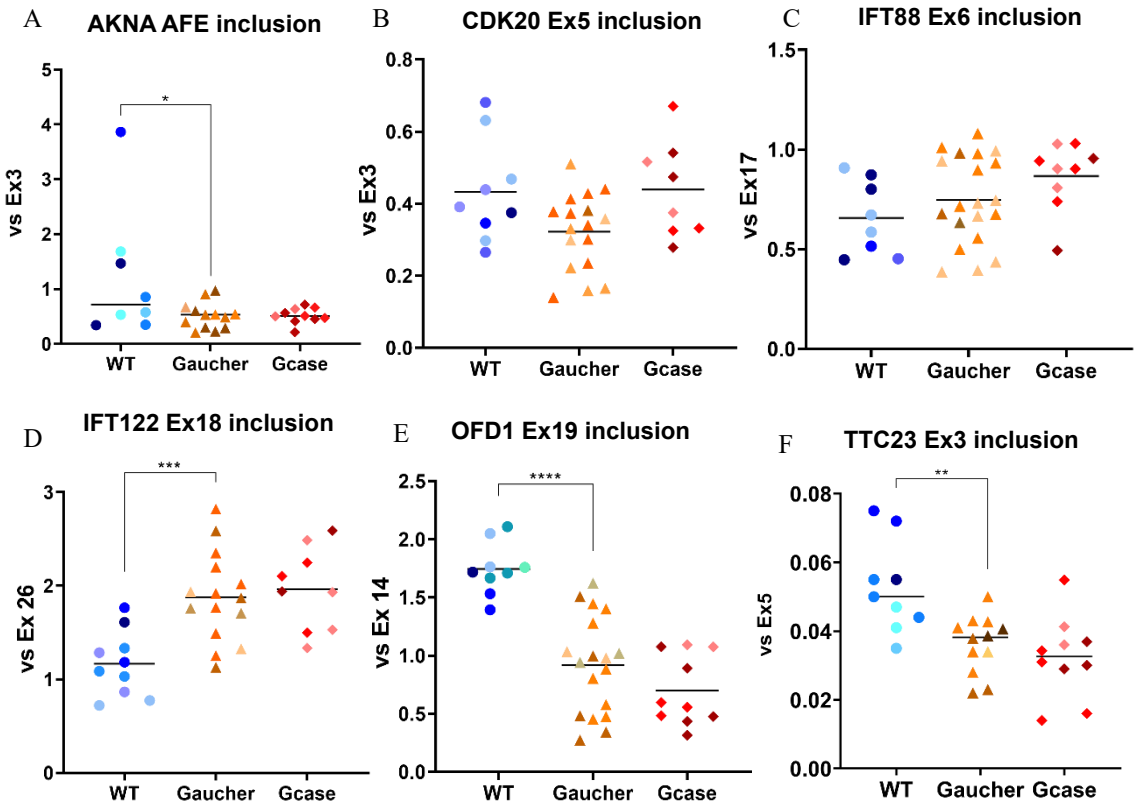

Figure 3.6. (A-F) Levels of inclusion of a subset of alternatively spliced exons in six ciliary transcripts in the experimental groups, WT in blue, Gaucher in orange and Gaucher + Gcase in red. **(A)** *AKNA AFE* (alternative first exon) inclusion against total *AKNA* Ex3. **(B)** *CDK20* Ex5 inclusion, normalized against total *CDK20* Ex3. **(C)** *IFT88* Ex6 inclusion, normalized against total *IFT88* Ex17. **(D)** *IFT122* Ex18 inclusion, normalized against total *IFT122* Ex26. **(E)** *OFD1* Ex19 inclusion, normalized against total *OFD1* Ex14. **(F)** *TTC23* Ex3 inclusion against total *TTC23* Ex5. A one-way ANOVA statistical test was performed between groups. *ρ-value < 0.5, ** ρ-value < 0.05, *** ρ-value < 0.01, **** ρ-value < 0.001.

Chapter 4. Discussion

This project aims to understand how lysosomal dysfunctions, in particular Gaucher disease, culminate in changes in the regulation of gene expression of ciliary genes and whether these changes are reversible after treatment with Gcase. Gaucher disease is caused by a mutation in the *GBA1* gene, which ultimately leads to an abnormal accumulation of glucosylceramide inside the lysosomes[8]. One of the treatments used is ERT with recombinant Gcase, namely Imiglucerase used throughout this study[13]. Cilia are structures with a chemical and mechanical sensory function, essential for the correct functioning of the cell due to their participation in the regulation of various signalling pathways[26,29,45]. These organelles have a well-defined length that when altered leads to dysregulations in the functioning of the cell[26,29,45].

In this work, we observe an increase in the length of the cilia of Gaucher primary fibroblasts compared to WT ones, a phenotype that was reversed upon Gcase treatment. We also verified, in Gaucher cilia, changes in acetylated α-tubulin distribution pattern, namely a decrease in the frequency of cilia with a continuous Arl13b staining and colocalization of the two proteins up to the ciliary tip, a phenotype that after treatment with Gcase show a slightly tendency to be revert to the WT one, where both proteins co-localize up to the ciliary tip continually.

Based on the literature, it is known that the ciliary length is defined at the end of ciliogenesis, this being a process regulated by two mechanisms: (1) the first one involves intraflagellar transport molecules, where it was found that an increase in the activity of anterograde transport leads to an increase in ciliary length whereas a decrease in its activity leads to smaller cilia and (2) a second one that involves posttranslational modifications of tubulin, mainly α-tubulin acetylation[67,68]. Thus, the changes in ciliary length observed in primary cilia from Gaucher patient' fibroblasts may be directly related to changes in the acetylation process of α-tubulin as morphological changes were observed in the axoneme of primary Gaucher cilia through staining with the anti-acetylated alpha tubulin antibody, namely with the acetylated tubulin not extending to the tip of the cilia in a considerable percentage of cells in this cell population.

The morphological changes in the cilium axoneme of Gaucher fibroblasts are accompanied by morphological changes in the ciliary membrane through the Arl13b staining, namely the appearance of cilia with an intermittent Arl13b staining, which may be caused by the deregulation of the interaction of Arl13b with acetylated α-tubulin. Arl13b is a GTPase, highly enriched in the ciliary membrane, being essential in the formation and maintenance of the primary cilium through the regulation of intraflagellar transport and the lipid composition of the ciliary membrane[49,66]. Previous studies found that Arl13b interacts with tubulin, namely acetylated α-tubulin, present in the cilium axoneme, with the aim of regulating the distribution of ciliary proteins along the ciliary membrane[69]. Considering that in previous studies changes in the levels of acetylated α-tubulin were observed in the absence of Arl13b, we can postulate that the deregulation of Arl13b observed in Gaucher cells leads to the deregulation of acetylated α-tubulin, causing changes in the ciliary membrane accompanied by changes in the axoneme[69].

Through the changes observed in acetylated α-tubulin pattern observed in the axoneme of primary cilia in Gaucher, it is possible to reinforce the relationship between Gaucher disease and Parkinson's. The acetylation process of α-tubulin is responsible for regulating the stability, dynamics and increase of the useful pathway of microtubules, these structures are present in nerve cells where they play an important role in transporting cargo between neurons, thus microtubules are essential for a correct communication between neuronal cells[20]. Previous studies have found that dysregulations of the

α-tubulin acetylation process contribute to the development of the neurodegenerative process, contributing to the appearance of many neurodegenerative diseases such as Parkinson's[20]. This suggests that similar to the alterations observed in the α-tubulin acetylation process in primary cilia from Gaucher patients, the α-tubulin acetylation process is also deregulated in primary cilia from Parkinson's disease.

Although this study is the first to attempt to establish a relationship between the primary cilium and Gaucher disease, this relationship had previously been established in two other studies performed in another lysosomal storage disease, Niemann-Pick type C1 (NPC1), an autosomal recessive lysosomal disease that leads to the accumulation of cholesterol in lysosomes[70]. In both studies, the authors found a decrease in the length of NPC1 primary cilia compared to fibroblasts from apparently healthy individuals, which was reversed upon 2-hydroxypropyl-b-cyclodextrin treatment, a drug used in the treatment of NPC1 disease[70,71]. Although we observed an increase in ciliary length in Gaucher fibroblasts, we can state that the results obtained in Gaucher fibroblasts are in line with those observed in the primary cilia in Niemann-Pick type C, as we also observed morphological changes in the primary cilium in Gaucher and a rescue of ciliary length after treatment with Gcase. Despite both NPC1 and Gaucher being lysosomal storage diseases, the molecular mechanisms behind the two diseases differ. In fact, based in the experimental data obtained by us and others, we may postulate that an increase in the activity of anterograde transport that culminates with longer cilia may be occurring in Gaucher fibroblasts, whereas a decrease in its activity may be responsible for the shorter cilia observed in NPC1 cilia. Further studies will be required to confirm such hypotheses.

Gaucher disease is caused by a mutation in the *GBA1* gene, that encodes the enzyme glucocerebrosidase responsible for the degradation of glucosylceramide into glucose and ceramide[8]. Thus, when there is a loss-of-function mutation in the *GBA1* gene, there is an inefficient degradation of glucosylceramide into glucose and ceramide[9]. As mentioned in the introduction, ceramide is one of the sphingolipids highly enriched in the ciliary membrane, playing an important role in regulating ciliogenesis, and previous studies have found that the reduction of ceramide inhibits ciliogenesis[22,35]. Ceramide can be synthesized through 3 mechanisms, (1) *de novo*: occurs in the endoplasmic reticulum, where serine palmitoyltransferase catalyzes the condensation of serine and palmitoyl-CoA to produce 3-ketosphinganine, which is then reduced to dehydroceremide serving as a precursor to ceramide; (2) hydrolysis of sphingomyelin occurs in the lysosomal membrane and plasma membrane, where the enzyme sphingomyelinase hydrolyzes sphingomyelin into ceramide; notice that, activation of sphingomyelinase occurs when the cell is under stress, causing this pathway to occur quickly; (3) salvage pathway: occurs mainly in lysosomes, where ceramide is formed through the degradation of complex sphingolipids, such as glycosphingolipids (glucosylceramide and shingomyelin). This mechanism requires the participation of several enzymes, and deregulations in these enzymes lead to lysosomal diseases causing a dysfunction in the salvage pathway[72,73].

In Gaucher, the lysosomal enzyme glucocerebrosidase, present in the ceramide synthesis mechanism, is deregulated, meaning that ceramide synthesis, through the salvage pathway, is not being synthesized correctly[8,73]. Based on the literature, we would expect to observe a decrease in the length of primary cilia of Gaucher fibroblasts, but indeed we observed an increase in ciliary length why? Ceramide synthesis mechanisms adapt to changes in cellular stress, particularly in cancer with cancer cells maintain low levels of ceramide, through increased ceramide turnover or ceramide storage, and in stroke patients, where increased ceramide levels are produced by *de novo* pathway[73,74]. We do not know the mechanism that led to the increase in ciliary length, but we may suggest that the deregulation in ceramide synthesis in the salvage pathway present in Gaucher disease leads to a hyperactivation in the remaining ceramide synthesis mechanisms, culminating to the longer cilia observed in Gaucher fibroblasts.

Interestingly, the sonic hedgehog (*Shh*) signaling pathway has been shown to be associated with the primary cilium, with this organelle being essential in *Shh* activation since PTCH1, GLI1 and SMO proteins are highly enriched in the ciliary membrane[24,50]. Thus, changes in the lipid composition and morphology of the primary cilium, namely in its membrane, may lead to *Shh* signaling pathway dysregulation[53]. The same previous studies performed in fibroblasts from NPC1 patients, where morphological changes in the primary cilium of such fibroblasts were reported, also state alterations in the *Shh* signaling pathway, namely a reduction in the expression of the PTCH1 protein and an increase in the *GLI1* protein that were, reversed in one of the studies through treatment with 2-hydroxypropyl-b-cyclodextrin[70,71]. Contrary to what was described in the previous works, without the addition of SAG, we did not observe changes in the activation of the *Shh* signaling pathway, with the expression levels of PTCH1 and GLI1 proteins being identical in Gaucher and WT fibroblasts. However, upon SAG treatment, there is a significant increase in the expression levels of both PTCH1 and GLI1 genes in Gaucher cells when compared with WT ones, meaning that there is a hyperactivation of the *Shh* signaling pathway in the Gaucher cells that is not reversed upon Gcase treatment. The authors of studies performed in fibroblasts from NPC1 patients suggest that the changes observed in the *Shh* signaling pathway may be related to the deregulation of cholesterol metabolism present in NPC1 patients[70]. Cholesterol is related to the Sonic Hedgehog signaling pathway, as cholesterol can directly activate Smo[75]. On the other hand, PTCH1 can bind to cholesterol, transporting it from the outer to the inner leaflet of the cell membrane, thus regulating the cholesterol available to activate Smo[75,76]. In Gaucher disease, contrary to what is observed in NPC1 patients, there is no such type of deregulation in cholesterol levels, so we can suggest that we did not see changes in *Shh* activation levels as cholesterol is not deregulated in Gaucher. Nevertheless, the morphological alterations observed in the ciliary membrane of Gaucher fibroblasts, namely its increased in size, may contribute for a higher number of receptors that could explain the hyperactivation of this signaling pathway.

Moreover, the validation by qRT-PCR of alternative splicing events in six ciliary genes (*AKNA, CDK20, IFT88, IFT122, OFD1* and *TTC23*), previously identified by RNA sequencing as being differentially alternatively spliced in Gaucher versus WT fibroblasts, suggests changes in the regulation of genetic expression of ciliary genes in Gaucher disease. Both *AKNA* and *OFD1* genes code for centrosomal proteins: *AKNA* codes for the microtubule organization protein *AKNA* that is responsible for the centrosomal organization of microtubules and for their growth and nucleation, whereas *OFD1* codes for the centriole and centriolar satellite protein *OFD1* located in the centrosome and in the basal body of the primary cilium, playing a crucial role in its formation[77,78]. *TTC23* codes for the tetratricopeptide repeat protein 23 that plays a positive role in the regulation of *Shh* signaling pathway, the last one being a key mediator of many fundamental processes namely cell growth, patterning, and morphogenesis during embryonic development[79]. Interestingly, *CDK20* gene codes for cyclin-dependent kinase 20 that is essential in the intraflagellar transport process, namely in retrograde transport and in controlling the structure of the primary cilium by coordinating assembly of the ciliary membrane and axoneme, allowing *GLI2* to be properly activated in response to Shh signaling[80,81]. Also, *IFT122* and *IFT88* genes code for intraflagellar transport proteins; *IFT122*, as a component of the IFT complex A (IFT-A), a complex required for retrograde ciliary transport and entry into cilia of G protein-coupled receptors (GPCRs), it is required in ciliogenesis and ciliary protein trafficking, whereas *IFT88* positively regulates primary cilium biogenesis[82,83].

Our results show that in Gaucher fibroblasts, levels of inclusion of a subset of alternatively spliced exons in *AKNA, CDK20, IFT88, IFT122, OFD1* and *TTC23* ciliary transcripts are statistically different from the ones observed in WT cells, which could be responsible for the morphological changes observed in these cells. Surprisingly, after treatment of Gaucher fibroblasts with Gcase, although the

differences were not statistically significant, only *CDK20* transcripts demonstrate a tendency to switch to an alternative splicing pattern closer to the one observed in WT fibroblasts. We can suggest that treatment with Gcase for 5 days is not sufficient to verify a reversional of alternative splicing events and it is necessary to increase the time of treatment with the recombinant enzyme.

Taking all these data in consideration, we may consider the *CDK20* gene as a strong candidate to explain some of the morphological changes observed in primary cilia in Gaucher fibroblasts. Previous studies have shown that changes in the *CDK2*0 gene cause an increase in ciliary length and an abnormal accumulation of ciliary proteins, such as IFT, in the ciliary tip [80,81]. On the other hand, *CDK20* was found, through interaction with *TBC1D32/BROMI*, to control both the structure of the primary cilium, the ciliary membrane and the axoneme, as well as the *Shh* signalling pathway[80,81]. Thus, lower levels of inclusion of exon 5 in *CDK20* transcripts in Gaucher fibroblasts may be responsible for the generation of CDK20 proteins that lead to an increase in ciliary length[80].

This project showed changes in the morphology of the primary cilium in Gaucher fibroblasts, namely the appearance of cilia with intermittent Arl13b staining and with an increased length. Moreover, Gcase treatment was able to rescue the ciliary length phenotype and recovered 49% of normal cilia morphology, bringing it closer to the values observed in WT. On the other hand, we identified changes in the acetylation process of α-tubulin which cause dysfunctions in the axoneme of the primary cilium in Gaucher cells. Interestingly, we identified a possible candidate responsible for the morphological changes of cilia observed in Gaucher fibroblasts, the *CDK20* gene, which showed a differential alternative splicing pattern when compared with the one presented in WT ones.

Even if we were unable to clarify the exact molecular mechanism by which lysosomal changes observed in Gaucher fibroblasts lead to changes in the primary cilium, and further studies will be required, the present study was the first one to pinpoint a link between primary cilia and Gaucher disease.

Chapter 5. References

1. Platt, F. M., d'Azzo, A., Davidson, B. L., Neufeld, E. F. & Tifft, C. J. Lysosomal storage diseases. *Nature Reviews Disease Primers* vol. 4, 27 Preprint at https://doi.org/10.1038/s41572-018-0025-4 (2018).

2. Parenti G, Medina DL, Ballabio A. The rapidly evolving view of lysosomal storage diseases. EMBO Mol Med. 2021 Feb 5;13(2):e12836. doi: 10.15252/emmm.202012836. Epub 2021 Jan 18. PMID: 33459519; PMCID: PMC7863408.

3. Settembre, C., Fraldi, A., Medina, D. L. & Ballabio, A. Signals from the lysosome: A control centre for cellular clearance and energy metabolism. *Nature Reviews Molecular Cell Biology* vol. 14 283–296 Preprint at https://doi.org/10.1038/nrm3565 (2013).

4. Marques ARA, Saftig P. Lysosomal storage disorders - challenges, concepts and avenues for therapy: beyond rare diseases. J Cell Sci. 2019 Jan 16;132(2):jcs221739. doi: 10.1242/jcs.221739. PMID: 30651381.

5. Parenti, G., Andria, G. & Ballabio, A. Lysosomal storage diseases: From pathophysiology to therapy. *Annu Rev Med* **66**, 471–486 doi: 10.1146/annurev-med-122313-085916. PMID: 25587658. (2015).

6. Suzuki Y. Chaperone therapy for molecular pathology in lysosomal diseases. Brain Dev. 2021 Jan;43(1):45-54. doi: 10.1016/j.braindev.2020.06.015. Epub 2020 Jul 29. PMID: 32736903.

7. Keyzor, I.; Shohet, S.; Castelli, J.; Sitaraman, S.; Veleva-Rotse, B.; Weimer, J.M.; Fox, B.; Willer, T.; Tuske, S.; Crathorne, L.; et al. Therapeutic Role of Pharmacological Chaperones in Lysosomal Storage Disorders: A Review of the Evidence and Informed Approach to Reclassification. Biomolecules 2023, 13, 1227. https://doi.org/10.3390/biom13081227

8. Nagral, A. Gaucher disease. *J Clin Exp Hepatol* **4**, 37–50 (2014) doi: 10.1016/j.jceh.2014.02.005. Epub 2014 Apr 21. PMID: 25755533; PMCID: PMC4017182..

9. Abed Rabbo, M., Khodour, Y., Kaguni, L. S. & Stiban, J. Sphingolipid lysosomal storage diseases: from bench to bedside. *Lipids in Health and Disease* vol. 20,44 Preprint at https://doi.org/10.1186/s12944-021-01466-0 (2021).

10. Arévalo NB, Lamaizon CM, Cavieres VA, Burgos PV, Álvarez AR, Yañez MJ, Zanlungo S. Neuronopathic Gaucher disease: Beyond lysosomal dysfunction. Front Mol Neurosci. 2022 Aug 3;15:934820. doi: 10.3389/fnmol.2022.934820. PMID: 35992201; PMCID: PMC9381931.

11. Hassanin, F., Abbas, A., Schalaan, M., Rabea, M. (2022). 'Gaucher disease: Recent advances in the diagnosis and management.', Medical Journal of Viral Hepatitis, 6.2(2), pp. 6-10. doi: 10.21608/mjvh.2022.234477.

12. Stirnemann J, Belmatoug N, Camou F, Serratrice C, Froissart R, Caillaud C, Levade T, Astudillo L, Serratrice J, Brassier A, Rose C, Billette de Villemeur T, Berger MG. A Review of Gaucher Disease Pathophysiology, Clinical Presentation and Treatments. Int J Mol Sci. 2017 Feb 17;18(2):441. doi: 10.3390/ijms18020441. PMID: 28218669; PMCID: PMC5343975.

13. Serratrice C, Carballo S, Serratrice J, Stirnemann J. Imiglucerase in the management of Gaucher disease type 1: an evidence-based review of its place in therapy. Core Evid. 2016 Oct 14;11:37-47. doi: 10.2147/CE.S93717. PMID: 27790078; PMCID: PMC5072572.

14. Annex I summary of Product Characteristics - European Medicines Agency (no date) europa.eu. Available at: https://www.ema.europa.eu/en/documents/product-information/cerezyme-epar-product-information_en.pdf (Accessed: 18 August 2023).

15. Onyenwoke RU, Brenman JE. Lysosomal Storage Diseases-Regulating Neurodegeneration. J Exp Neurosci. 2016 Apr 5;9(Suppl 2):81-91. doi: 10.4137/JEN.S25475. PMID: 27081317; PMCID: PMC4822725.16. Ferguson, S. M. Neuronal lysosomes. *Neuroscience Letters* vol. 697 1–9 Preprint at https://doi.org/10.1016/j.neulet.2018.04.005 (2019).

17. Di Rocco, M., Di Fonzo, A., Barbato, A. et al. Parkinson's disease in Gaucher disease patients: what's changing in the counseling and management of patients and their relatives?. Orphanet J Rare Dis 15, 262 (2020). https://doi.org/10.1186/s13023-020-01529-y

18. Blanz J, Saftig P. Parkinson's disease: acid-glucocerebrosidase activity and alpha-synuclein clearance. J Neurochem. 2016 Oct;139 Suppl 1:198-215. doi: 10.1111/jnc.13517. Epub 2016 Feb 10. PMID: 26860955.

19. Leyns, C.E.G., Prigent, A., Beezhold, B. et al. Glucocerebrosidase activity and lipid levels are related to protein pathologies in Parkinson's disease. npj Parkinsons Dis. 9, 74 (2023). https://doi.org/10.1038/s41531-023-00517-w

20. Naren, P., Samim, K.S., Tryphena, K.P. et al. Microtubule acetylation dyshomeostasis in Parkinson's disease. Transl Neurodegener 12, 20 (2023). https://doi.org/10.1186/s40035-023-00354-0

21. Mary Mirvis, Tim Stearns, W. James Nelson; Cilium structure, assembly, and disassembly regulated by the cytoskeleton. Biochem J 31 July 2018; 475 (14): 2329–2353. doi: https://doi.org/10.1042/BCJ20170453

22. Kaiser, F., Huebecker, M. & Wachten, D. Sphingolipids controlling ciliary and microvillar function. *FEBS Letters* vol. 594 3652–3667 Preprint at https://doi.org/10.1002/1873-3468.13816 (2020).

23. Wheway, G., Nazlamova, L. & Hancock, J. T. Signaling through the primary cilium. *Frontiers in Cell and Developmental Biology* vol. 6 Preprint at https://doi.org/10.3389/fcell.2018.00008 (2018).

24. Ho, E. K. & Stearns, T. Hedgehog signaling and the primary cilium: Implications for spatial and temporal constraints on signaling. *Development (Cambridge)* vol. 148 Preprint at https://doi.org/10.1242/dev.195552 (2021).

25. Yamamoto Y, Mizushima N. Autophagy and Ciliogenesis. JMA J. 2021 Jul 15;4(3):207-215. doi: 10.31662/jmaj.2021-0090. Epub 2021 Jul 6. PMID: 34414314; PMCID: PMC8355725.

26. Pala, R.; Jamal, M.; Alshammari, Q.; Nauli, S.M. The Roles of Primary Cilia in Cardiovascular Diseases. Cells 2018, 7, 233. https://doi.org/10.3390/cells7120233

27. He, K., Ling, K. & Hu, J. The emerging role of tubulin posttranslational modifications in cilia and ciliopathies. Biophys Rep 6, 89–104 (2020). https://doi.org/10.1007/s41048-020-00111-0

28. Wang, L., Wen, X., Wang, Z. et al. Ciliary transition zone proteins coordinate ciliary protein composition and ectosome shedding. Nat Commun 13, 3997 (2022). https://doi.org/10.1038/s41467-022-31751-0

29. Patel, M.M.; Tsiokas, L. Insights into the Regulation of Ciliary Disassembly. Cells 2021, 10, 2977. https://doi.org/10.3390/cells10112977

30. Wang W, Jack BM, Wang HH, Kavanaugh MA, Maser RL, Tran PV. Intraflagellar Transport Proteins as Regulators of Primary Cilia Length. Front Cell Dev Biol. 2021 May 19;9:661350. doi: 10.3389/fcell.2021.661350. PMID: 34095126; PMCID: PMC8170031.

31. Long H, Huang K. Transport of Ciliary Membrane Proteins. Front Cell Dev Biol. 2020 Jan 13;7:381. doi: 10.3389/fcell.2019.00381. PMID: 31998723; PMCID: PMC6970386.

32. Chen C, Hu J, Ling K. The Role of Primary Cilia-Associated Phosphoinositide Signaling in Development. J Dev Biol. 2022 Dec 2;10(4):51. doi: 10.3390/jdb10040051. PMID: 36547473; PMCID: PMC9785882.

33. Ferreira, Luisa & Figueiredo, Ana & Orr, Bernardo & Lopes, Danilo & Maiato, Helder. (2018). Dissecting the role of the tubulin code in mitosis. Doi: 10.1016/bs.mcb.2018.03.040.

34. Goetz SC, Anderson KV. The primary cilium: a signaling centre during vertebrate development. Nat Rev Genet. 2010 May;11(5):331-44. doi: 10.1038/nrg2774. PMID: 20395968; PMCID: PMC3121168.

35. Wu D, Huang J, Zhu H, Chen Z, Chai Y, Ke J, Lei K, Peng Z, Zhang R, Li X, Huang K, Li W, Zhao C, Ou G. Ciliogenesis requires sphingolipid-dependent membrane and axoneme interaction. Proc Natl Acad Sci U S A. 2022 Aug 2;119(31):e2201096119. doi: 10.1073/pnas.2201096119. Epub 2022 Jul 27. PMID: 35895683; PMCID: PMC9351462.

36. Carmona B, Marinho HS, Matos CL, Nolasco S, Soares H. Tubulin Post-Translational Modifications: The Elusive Roles of Acetylation. Biology (Basel). 2023 Apr 6;12(4):561. doi: 10.3390/biology12040561. PMID: 37106761; PMCID: PMC10136095.

37. Wloga D, Joachimiak E, Louka P, Gaertig J. Posttranslational Modifications of Tubulin and Cilia. Cold Spring Harb Perspect Biol. 2017 Jun 1;9(6):a028159. doi: 10.1101/cshperspect.a028159. PMID: 28003186; PMCID: PMC5453388.

38. Nekooki-Machida, Y., Hagiwara, H. Role of tubulin acetylation in cellular functions and diseases. Med Mol Morphol 53, 191–197 (2020). https://doi.org/10.1007/s00795-020-00260-8

39. Eshun-Wilson L, Zhang R, Portran D, Nachury MV, Toso DB, Löhr T, Vendruscolo M, Bonomi M, Fraser JS, Nogales E. Effects of α-tubulin acetylation on microtubule structure and stability. Proc Natl Acad Sci U S A. 2019 May 21;116(21):10366-10371. doi: 10.1073/pnas.1900441116. Epub 2019 May 9. PMID: 31072936; PMCID: PMC6535015.

40. van Niel, G., D'Angelo, G. & Raposo, G. Shedding light on the cell biology of extracellular vesicles. Nat Rev Mol Cell Biol 19, 213–228 (2018). https://doi.org/10.1038/nrm.2017.125

41. Vinay, L. & Belleannée, C. EV duty vehicles: Features and functions of ciliary extracellular vesicles. *Frontiers in Genetics* vol. 13 Preprint at https://doi.org/10.3389/fgene.2022.916233 (2022).

42. Long H, Zhang F, Xu N, Liu G, Diener DR, Rosenbaum JL, Huang K. Comparative Analysis of Ciliary Membranes and Ectosomes. Curr Biol. 2016 Dec 19;26(24):3327-3335. doi: 10.1016/j.cub.2016.09.055. Epub 2016 Nov 17. PMID: 27866888; PMCID: PMC5173405.

43. Razzauti A, Laurent P. Ectocytosis prevents accumulation of ciliary cargo in C. elegans sensory neurons. Elife. 2021 Sep 17;10:e67670. doi: 10.7554/eLife.67670. PMID: 34533135; PMCID: PMC8492061.

44. Hsu KS, Chuang JZ, Sung CH. The Biology of Ciliary Dynamics. Cold Spring Harb Perspect Biol. 2017 Apr 3;9(4):a027904. doi: 10.1101/cshperspect.a027904. PMID: 28062565; PMCID: PMC5378047.

45. Macarelli, V., Leventea, E. & Merkle, F. T. Regulation of the length of neuronal primary cilia and its potential effects on signaling. *Trends in Cell Biology* Preprint at https://doi.org/10.1016/j.tcb.2023.05.005 (2023).

46. He Q, Wang G, Dasgupta S, Dinkins M, Zhu G, Bieberich E. Characterization of an apical ceramide-enriched compartment regulating ciliogenesis. Mol Biol Cell. 2012 Aug;23(16):3156-66. doi: 10.1091/mbc.E12-02-0079. Epub 2012 Jun 20. PMID: 22718902; PMCID: PMC3418310.

47. Carballo, G. B., Honorato, J. R., De Lopes, G. P. F. & Spohr, T. C. L. D. S. E. A highlight on Sonic hedgehog pathway. *Cell Communication and Signaling* vol. 16 Preprint at https://doi.org/10.1186/s12964-018-0220-7 (2018).

48. Huangfu, D. & Anderson, K. V. Signaling from Smo to Ci/Gli: Conservation and divergence of Hedgehog pathways from Drosophila to vertebrates. *Development* vol. 133 3–14 Preprint at https://doi.org/10.1242/dev.02169 (2006).

49. Gigante ED, Taylor MR, Ivanova AA, Kahn RA, Caspary T. ARL13B regulates Sonic hedgehog signaling from outside primary cilia. Elife. 2020 Mar 4;9:e50434. doi: 10.7554/eLife.50434. PMID: 32129762; PMCID: PMC7075693.

50. Caspary T, Larkins CE, Anderson KV. The graded response to Sonic Hedgehog depends on cilia architecture. Dev Cell. 2007 May;12(5):767-78. doi: 10.1016/j.devcel.2007.03.004. PMID: 17488627.

51. Suchors, C. & Kim, J. Canonical Hedgehog Pathway and Noncanonical GLI Transcription Factor Activation in Cancer. *Cells* vol. 11 Preprint at https://doi.org/10.3390/cells11162523 (2022).

52. Lex RK, Zhou W, Ji Z, Falkenstein KN, Schuler KE, Windsor KE, Kim JD, Ji H, Vokes SA. GLI transcriptional repression is inert prior to Hedgehog pathway activation. Nat Commun. 2022 Feb 10;13(1):808. doi: 10.1038/s41467-022-28485-4. PMID: 35145123; PMCID: PMC8831537.

53. Bangs F, Anderson KV. Primary Cilia and Mammalian Hedgehog Signaling. Cold Spring Harb Perspect Biol. 2017 May 1;9(5):a028175. doi: 10.1101/cshperspect.a028175. PMID: 27881449; PMCID: PMC5411695.

54. Pietrobono, S., Gagliardi, S. & Stecca, B. Non-canonical hedgehog signaling pathway in cancer: Activation of GLI transcription factors beyond smoothened. *Frontiers in Genetics* vol. 10 Preprint at https://doi.org/10.3389/fgene.2019.00556 (2019).

55. Pusapati GV, Rohatgi R. Location, location, and location: compartmentalization of Hedgehog signaling at primary cilia. EMBO J. 2014 Sep 1;33(17):1852-4. doi: 10.15252/embj.201489294. Epub 2014 Jul 17. PMID: 25037564; PMCID: PMC4195781.

56. Wang Y, Liu J, Huang BO, Xu YM, Li J, Huang LF, Lin J, Zhang J, Min QH, Yang WM, Wang XZ. Mechanism of alternative splicing and its regulation. Biomed Rep. 2015 Mar;3(2):152-158. doi: 10.3892/br.2014.407. Epub 2014 Dec 17. PMID: 25798239; PMCID: PMC4360811.

57. Reble, E., Dineen, A. & Barr, C. L. The contribution of alternative splicing to genetic risk for psychiatric disorders. *Genes, Brain and Behavior* vol. 17 Preprint at https://doi.org/10.1111/gbb.12430 (2018).

58. Plaschka C, Newman AJ, Nagai K. Structural Basis of Nuclear pre-mRNA Splicing: Lessons from Yeast. Cold Spring Harb Perspect Biol. 2019 May 1;11(5):a032391. doi: 10.1101/cshperspect.a032391. PMID: 30765413; PMCID: PMC6496352.

59. Anna, A. & Monika, G. Splicing mutations in human genetic disorders: examples, detection, and confirmation. *Journal of Applied Genetics* vol. 59 253–268 Preprint at https://doi.org/10.1007/s13353-018-0444-7 (2018).

60. Hertel, K. J. Combinatorial control of exon recognition. *Journal of Biological Chemistry* vol. 283 1211–1215 Preprint at https://doi.org/10.1074/jbc.R700035200 (2008).

61. Le, K. Q., Prabhakar, B. S., Hong, W. J. & Li, L. C. Alternative splicing as a biomarker and potential target for drug discovery. *Acta Pharmacologica Sinica* vol. 36 1212–1218 Preprint at https://doi.org/10.1038/aps.2015.43 (2015).

62. Lam SD, Babu MM, Lees J, Orengo CA. Biological impact of mutually exclusive exon switching. PLoS Comput Biol. 2021 Mar 2;17(3):e1008708. doi: 10.1371/journal.pcbi.1008708. PMID: 33651795; PMCID: PMC7954323.

63. Ren, F., Zhang, N., Zhang, L., Miller, E. & Pu, J. J. Alternative Polyadenylation: a new frontier in post transcriptional regulation. *Biomarker Research* vol. 8 Preprint at https://doi.org/10.1186/s40364-020-00249-6 (2020).

64. Santos, J.I.; Gonçalves, M.; Matos, L.; Moreira, L.; Carvalho, S.; Prata, M.J.; Coutinho, M.F.; Alves, S. Splicing Modulation as a Promising Therapeutic Strategy for Lysosomal Storage Disorders: The Mucopolysaccharidoses Example. Life 2022, 12, 608. https://doi.org/10.3390/life12050608

65. Roberts, T. C., Langer, R. & Wood, M. J. A. Advances in oligonucleotide drug delivery. *Nature Reviews Drug Discovery* vol. 19 673–694 Preprint at https://doi.org/10.1038/s41573-020-0075-7 (2020).

66. Sztul E, Chen PW, Casanova JE, Cherfils J, Dacks JB, Lambright DG, Lee FS, Randazzo PA, Santy LC, Schürmann A, Wilhelmi I, Yohe ME, Kahn RA. ARF GTPases and their GEFs and GAPs: concepts and challenges. Mol Biol Cell. 2019 May 15;30(11):1249-1271. doi: 10.1091/mbc.E18-12-0820. PMID: 31084567; PMCID: PMC6724607.

67. Keeling, J., Tsiokas, L. & Maskey, D. Cellular mechanisms of ciliary length control. *Cells* vol. 5 Preprint at https://doi.org/10.3390/cells5010006 (2016).

68. Ishikawa H, Marshall WF. Intraflagellar Transport and Ciliary Dynamics. Cold Spring Harb Perspect Biol. 2017 Mar 1;9(3):a021998. doi: 10.1101/cshperspect.a021998. PMID: 28249960; PMCID: PMC5334256.

69. Revenkova E, Liu Q, Gusella GL, Iomini C. The Joubert syndrome protein ARL13B binds tubulin to maintain uniform distribution of proteins along the ciliary membrane. J Cell Sci. 2018 May 4;131(9):jcs212324. doi: 10.1242/jcs.212324. PMID: 29592971; PMCID: PMC5992585.

70. Canterini S, Dragotto J, Dardis A, Zampieri S, De Stefano ME, Mangia F, Erickson RP, Fiorenza MT. Shortened primary cilium length and dysregulated Sonic hedgehog signaling in Niemann-Pick C1 disease. Hum Mol Genet. 2017 Jun 15;26(12):2277-2289. doi: 10.1093/hmg/ddx118. PMID: 28379564.

71. Formichi P, Battisti C, De Santi MM, Guazzo R, Tripodi SA, Radi E, Rossi B, Tarquini E, Federico A. Primary cilium alterations and expression changes of Patched1 proteins in niemann-pick type C disease. J Cell Physiol. 2018 Jan;233(1):663-672. doi: 10.1002/jcp.25926. Epub 2017 May 19. PMID: 28332184.

72. Sokolowska, E. & Blachnio-Zabielska, A. The Role of Ceramides in Insulin Resistance. *Frontiers in Endocrinology* vol. 10 Preprint at https://doi.org/10.3389/fendo.2019.00577 (2019).

73. Yuan, H., Zhu, B., Li, C. & Zhao, Z. Ceramide in cerebrovascular diseases. *Frontiers in Cellular Neuroscience* vol. 17 Preprint at https://doi.org/10.3389/fncel.2023.1191609 (2023).

74. Stith, J. L., Velazquez, F. N. & Obeid, L. M. Advances in determining signaling mechanisms of ceramide and role in disease. *Journal of Lipid Research* vol. 60 913–918 Preprint at https://doi.org/10.1194/jlr.S092874 (2019).

75. Kinnebrew M, Iverson EJ, Patel BB, Pusapati GV, Kong JH, Johnson KA, Luchetti G, Eckert KM, McDonald JG, Covey DF, Siebold C, Radhakrishnan A, Rohatgi R. Cholesterol accessibility at the ciliary membrane controls hedgehog signaling. Elife. 2019 Oct 30;8:e50051. doi: 10.7554/eLife.50051. PMID: 31657721; PMCID: PMC6850779.

76. Xu, S. & Tang, C. Cholesterol and Hedgehog Signaling: Mutual Regulation and Beyond. *Frontiers in Cell and Developmental Biology* vol. 10 Preprint at https://doi.org/10.3389/fcell.2022.774291 (2022).

77. Camargo Ortega G, Falk S, Johansson PA, Peyre E, Broix L, Sahu SK, Hirst W, Schlichthaerle T, De Juan Romero C, Draganova K, Vinopal S, Chinnappa K, Gavranovic A, Karakaya T, Steininger T, Merl-Pham J, Feederle R, Shao W, Shi SH, Hauck SM, Jungmann R, Bradke F, Borrell V, Geerlof A, Reber S, Tiwari VK, Huttner WB, Wilsch-Bräuninger M, Nguyen L, Götz M. The centrosome protein AKNA regulates neurogenesis via microtubule organization. Nature. 2019 Mar;567(7746):113-117. doi: 10.1038/s41586-019-0962-4. Epub 2019 Feb 20. PMID: 30787442.

78. Pezzella, N., Bove, G., Tammaro, R. & Franco, B. OFD1: One gene, several disorders. *American Journal of Medical Genetics, Part C: Seminars in Medical Genetics* vol. 190 57–71 Preprint at https://doi.org/10.1002/ajmg.c.31962 (2022).

79. Shamseldin HE, Shaheen R, Ewida N, Bubshait DK, Alkuraya H, Almardawi E, Howaidi A, Sabr Y, Abdalla EM, Alfaifi AY, Alghamdi JM, Alsagheir A, Alfares A, Morsy H, Hussein MH, Al-Muhaizea MA, Shagrani M, Al Sabban E, Salih MA, Meriki N, Khan R, Almugbel M, Qari A, Tulba M, Mahnashi M, Alhazmi K, Alsalamah AK, Nowilaty SR, Alhashem A, Hashem M, Abdulwahab F, Ibrahim N, Alshidi T, AlObeid E, Alenazi MM, Alzaidan H, Rahbeeni Z, Al-Owain M, Sogaty S, Seidahmed MZ, Alkuraya FS. The morbid genome of ciliopathies: an update. Genet Med. 2020 Jun;22(6):1051-1060. doi: 10.1038/s41436-020-0761-1. Epub 2020 Feb 14. Erratum in: Genet Med. 2022 Apr;24(4):966. PMID: 32055034.

80. Satoda Y, Noguchi T, Fujii T, Taniguchi A, Katoh Y, Nakayama K. BROMI/TBC1D32 together with CCRK/CDK20 and FAM149B1/JBTS36 contributes to intraflagellar transport turnaround involving ICK/CILK1. Mol Biol Cell. 2022 Aug 1;33(9):ar79. doi: 10.1091/mbc.E22-03-0089. Epub 2022 May 24. PMID: 35609210; PMCID: PMC9582636.

81. Noguchi T, Nakamura K, Satoda Y, Katoh Y, Nakayama K. CCRK/CDK20 regulates ciliary retrograde protein trafficking via interacting with BROMI/TBC1D32. PLoS One. 2021 Oct 8;16(10):e0258497. doi: 10.1371/journal.pone.0258497. PMID: 34624068; PMCID: PMC8500422.

82. Lee J, Yi S, Won M, Song YS, Yi HS, Park YJ, Park KC, Kim JT, Chang JY, Lee MJ, Sul HJ, Choi JE, Kim KS, Kero J, Kim J, Shong M. Loss-of-function of IFT88 determines metabolic phenotypes in thyroid cancer. Oncogene. 2018 Aug;37(32):4455-4474. doi: 10.1038/s41388-018-0211-6. Epub 2018 May 10. PMID: 29743590.

83. Qin J, Lin Y, Norman RX, Ko HW, Eggenschwiler JT. Intraflagellar transport protein 122 antagonizes Sonic Hedgehog signaling and controls ciliary localization of pathway components. Proc Natl Acad Sci U S A. 2011 Jan 25;108(4):1456-61. doi: 10.1073/pnas.1011410108. Epub 2011 Jan 5. PMID: 21209331; PMCID: PMC3029728.

Appendix I – List of the sequence of primers used

Table II. Detailed sequences of the primers used in the analysis of alternative splicing event.

Name	Gene	Amplicon size (bp)	Sequence	Position (cDNA)	Event analysed
AKNA AFE Fw	AKNA	129	AGGTGCCCAAGGTCAGAAG	Ex1	Inclusion of AKNA first exon
AKNA Ex2 Rv			ACCTGGGCCACTTCATCTT	Ex2	
AKNA Ex3 Fw		165	CCACTCCCTGATTTCTCCAA	Ex3	
AKNA Ex3 Rv			ACTGCTCAACAGCACCTCCT		
TTC23 Ex3 Fw	TTC23	120	TGAAATTTTAAGCCCCAGCTA		Inclusion of TTC23 exon 3
TTC23 Ex4 Rv			ACCTCAGCTCAGGAGTTTGG	Ex4	
TTC23 Ex5 Fw		156	TGCAAGAATCACAGGAAACC	Ex5	
TTC23 Ex5 Rv			TTGCTTTCTCTTCACAGAGGTG		
IFT88 Ex6 Fw	IFT88	97	AAAATATCAAGCACGGCAGTT	Ex6	Inclusion of IFT88 exon 6
IFT88 Ex7 Rv			TAGCCCCTGTCATTGGTCTT	Ex7	
IFT88 Ex17 Fw		100	GTGCGTGGAAGTGGTGAAAG	Ex17	
IFT88 Ex17 Rv			TTGGTTATAGTCTTTTTGTCTCAAGTA		
CDK20 Ex5 Fw	CDK20	133	GTATGGTGCCCGCCAGTAT	Ex5	Inclusion of CDK20 exon 5
CDK20 Ex6 Rv			GATGCGAAGCACATAGCAAA	Ex6	
CDK20 Ex3 Fw		151	ACAACTGAAGGCTGTGTTCC	Ex3	
CDK20 Ex3 Rv			GACACCCTTGAGCAGCATCT		
IFT122 Ex17 Fw	IFT122	156	TGTTCAAGGAAGCCTACCAGA	Ex17	Inclusion of IFT122 exon 18
IFT122 Ex18 Rv			TGCTGCTGATGAGCTCTAAA	Ex18	
IFT122 Ex26 Fw		157	CAAGGTGGCTCAGAGTTCGT	Ex26	
IFT122 Ex26 Rv			AGGAGGGGCACATGGTAAT		
OFD1 Ex19 Fw	OFD1	156	CGGGGATATGTCTCATGTGG	Ex19	Inclusion of OFD1 exon 19
OFD1 Ex20 Rv			TGCCTTCTTTCTTCTCTCTGC	Ex20	
OFD1 Ex14 Fw		116	GGCTCCTGAACTTGCAGTCT	Ex14	
OFD1 Ex14 Rv			CGTCTTGCAGTTGTTTGTGC		